

SGD May Never Escape Saddle Points

Liu Ziyin¹, Botao Li², James B. Simon³, and Masahito Ueda¹

¹*Department of Physics, University of Tokyo*

²*Laboratoire de Physique de l'Ecole normale supérieure, ENS, Université PSL, CNRS, Sorbonne Université, Université Paris-Diderot, Sorbonne Paris Cité*

³*Department of Physics and Redwood Center For Theoretical Neuroscience, University of California, Berkeley*

June 11, 2022

Abstract

Stochastic gradient descent (SGD) has been deployed to solve highly non-linear and non-convex machine learning problems such as the training of deep neural networks. However, previous works on SGD often rely on restrictive and unrealistic assumptions about the nature of noise in SGD. In this work, we mathematically construct examples that defy previous understandings of SGD. For example, our constructions show that: (1) SGD may converge to a local maximum; (2) SGD may escape a saddle point arbitrarily slowly; (3) SGD may prefer sharp minima over the flat ones; and (4) AMSGrad may converge to a local maximum. We also show the relevance of our result to deep learning by presenting a minimal neural network example. Our result suggests that the noise structure of SGD might be more important than the loss landscape in neural network training and that future research should focus on deriving the actual noise structure in deep learning.

1 Introduction

SGD is the main optimization algorithm underpinning the success of deep learning, and understanding SGD is widely regarded as one major step towards understanding deep learning (Bottou, 2012; Zhang et al., 2018; Xing et al., 2018; Mori et al., 2021; Du et al., 2018; Allen-Zhu et al., 2018; Wojtowysch, 2021a,b; Gower et al., 2021; Ziyin et al., 2021; Gurbuzbalaban et al., 2021; Zou et al., 2021; Li et al., 2021; Feng and Tu, 2021). Despite its algorithmic simplicity (describable with only two lines of equations), SGD is hard to understand. The challenge is threefold: (1) SGD is discrete-time in nature, and discrete-time dynamics are known to lead to much more complicated dynamics than their continuous-time counterpart (May, 1976); (2) SGD noise is multiplicative and state-dependent (Ziyin et al., 2021; Hodgkinson and Mahoney, 2020); and (3) the loss landscape can be non-linear and non-convex, containing many local minima, saddle points, and degeneracies in the landscape (Xing et al., 2018; Wu et al., 2017). Each of these challenges is so difficult that very few works attempt to deal with all three simultaneously. Most previous works of SGD are limited to the cases when the loss landscape is strongly convex (Ziyin et al., 2021; Liu et al., 2021; Hoffer et al., 2017; Mandt et al., 2017), or when the noise is assumed to be Gaussian and time-independent (Zhu et al., 2019; Jastrzebski et al., 2017; Xie et al., 2021); for the works that tackle SGD in a non-convex setting, often strong conditions are assumed. The reliance on strong assumptions regarding each of the challenges means that our present understanding of SGD for deep learning is speculative. This work aims to examine some commonly held presumptions about SGD and show that when all the three challenging factors are taken together, many counter-intuitive phenomena may happen, in direct contrast to commonly held speculations about SGD.

In this work, we study the behavior of SGD in a landscape with non-convex loss and multi-minima. The focus of this work is the direct opposite to that of many related works: instead of showing when SGD will converge, we set out to answer the question of when SGD does not. We study the behavior of discrete-time

SGD close to a saddle point; the noise is due to minibatch sampling; the learning rate is held constant throughout training, which resembles the actual training setting more than the common assumption that the learning rate is decreased through time. The main **contributions** of this work are the following:

1. We show that the noise in SGD may cause SGD to be attracted to local maxima and saddle points, contrary to the previous premise that SGD can overcome loss landscape barriers easily;
2. Additionally, we show that, even if one can tune the learning rate of SGD freely to escape a saddle point, there exist cases where SGD may take arbitrarily long to escape, independent of parameter tuning;
3. We show that the widespread belief that SGD prefers flat minima does not hold by explicitly constructing an example where SGD converges to a sharp minimum in probability, independent of initialization;
4. We show that our result can also be extended to other stochastic optimizers; in particular, we show that, on a non-convex landscape, AMSgrad may also not converge (and converge to a local maximum instead), contrary to the widely held belief that Amsgrad is the “convergent” version of Adam.

2 Background

In this section, we introduce the minibatch SGD algorithm. The objective for SGD can be defined as a pair $(\hat{L}, p(x))$ such that \hat{L} is a differentiable function and $p(x)$ is a probability density. We are concerned with finding the minimizer of the following differentiable objective:

$$L(w) = \mathbb{E}_{x \sim p(x)}[\hat{L}(w; x)] \quad (1)$$

where x is a data point drawn from distribution $p(x)$ and $w \in \mathbb{R}^D$ is the model parameter. We can define the gradient descent (GD) algorithm for L as $w_t = w_{t-1} - \lambda \nabla_w L(w, x)$ for some randomly initialized w_0 , where λ is the learning rate. In this definition, the minibatch SGD algorithm can be defined.

Definition 1. *The minibatch SGD algorithm by sampling with replacement computes the update to the parameter w with the following set of equations:*

$$\begin{cases} \hat{g}_t = \nabla \hat{L}(w_{t-1}; x_t); \\ w_t = w_{t-1} - \lambda \hat{g}_t. \end{cases} \quad (2)$$

where x_t is drawn from $p(x)$ such that x_i is independent of x_j for $i \neq j$.

This is equivalent to the SGD algorithm with minibatch size 1, which is also relevant to an online learning setting. When the batch size is large, it is often the case that the gradient distribution converges to a colored multivariate Gaussian by the law of large numbers (Zhiyi and Ziyin, 2021; Xie et al., 2021). We briefly consider the case of Gaussian noise in the appendix Section B.2. While we focus on analyzing discrete-time SGD in the main text, we note that part of our result can also be derived in the continuous-time limit, which we present in the appendix Section C.¹

Notation and Terminology. We use λ to denote the learning rate. w is the model parameter. $\hat{L}(w; x)$, with the $\hat{\cdot}$, denotes the *sampled* loss function, which is a function of the data point, and $L := \mathbb{E}_x[\hat{L}]$; for notational conciseness, we often hide the dependence on x when the context is clear. The lowercase t denotes the time step of optimization. In this work, the terms *learning rate* and *step size* are used interchangeably. The phrases *loss*, *objective*, and *potential* are also used interchangeably.

¹While the limitation of continuous-time approximation is that it only applies approximately when λ is small, the advantage is that the result is now independent of the distribution of the gradient (and only depend on the gradient covariance).

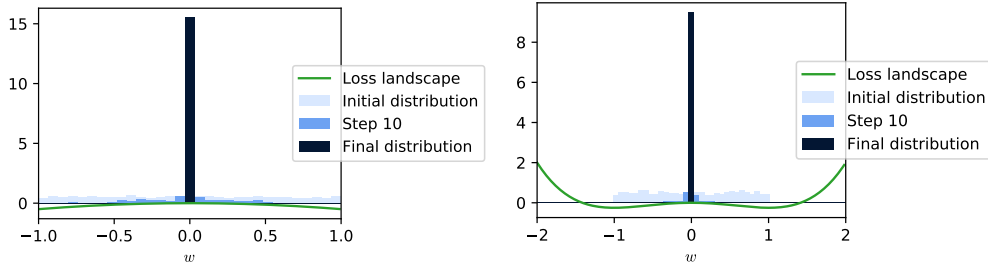


Figure 1: Distribution of the parameter w , initialized uniformly in the interval $[-1, 1]$. We see that, for both the quadratic potential and the fourth order potential, a concentration of measure is observed, namely, we see that SGD converges to a local maximum. **Left:** Distribution of w on the quadratic potential, $\hat{L} = xw^2/2$, studied in Section 5.1. **Right:** Distribution on the fourth order potential, $\hat{L} = xw^2/2 + w^4$.

3 Related Works

Escaping Saddle Points. Because neural networks are highly non-linear, the landscape of neural networks is believed to contain many local minima and saddle points (Du et al., 2017; Kleinberg et al., 2018; Reddi et al., 2018b). It is thus crucial for any optimization algorithm to be able to overcome saddle points efficiently and not become stuck in a suboptimal minimum. However, the majority of works on escaping saddle points assumes no stochasticity or only artificially injected noise (Du et al., 2017; Jin et al., 2017; Ge et al., 2015; Reddi et al., 2018b; Lee et al., 2016). Some physics-inspired approaches take the stochasticity into account but often rely on continuous-time approximation and hard-to-justify assumptions regarding the stationary distribution of the parameter (Mori et al., 2021; Xie et al., 2021; Liu et al., 2021). A few works that do consider the stochasticity in finite step-size SGD rely on strong assumptions about the noise, whose relevance to deep learning are not clear (see the next paragraph).

Role of Minibatch Noise. Until now, the dominant trend of SGD research has been about analyzing SGD on various landscapes. However, one indispensable aspect of SGD is its special stochasticity due to minibatch sampling (Ziyin et al., 2021; Zhu et al., 2019), whose strength and structure are only determined by the model architecture and the distribution of the data points. It is handy to decompose the gradient into an expectation part and a fluctuation part:

$$\hat{g}_t = g_t + \sqrt{C}\eta_t \quad (3)$$

where η_t is a random variable such that $\text{cov}(\eta_t, \eta_{t'}) = \delta_{t,t'}I$ with I being the identity matrix and $\delta_{t,t'}$ being the Kronecker’s delta; $g_t = \mathbb{E}[\hat{g}_t]$ is the gradient of GD, and C is the SGD noise covariance. Recent works show that $C = C(w_t)$ crucially depends on the model parameter w_t , which has a significant effect on the convergence and dynamics of SGD (Hodgkinson and Mahoney, 2020). In fact, it has been shown that the models trained with SGD significantly outperform the models directly trained with GD (Hoffer et al., 2017), which suggests that minibatch noise in SGD is beneficial for training. Understanding the role of minibatch noise is therefore of both fundamental and practical value. However, in the previous works, the focus is on analyzing the behavior of SGD on the landscape specified by L ; the unique structures due to the noise in SGD are often treated in an oversimplified manner without referring to the actual models in deep learning or the actual data distributions. For example, Daneshmand et al. (2018) assumes that the noisy gradient is negatively correlated with the direction of the Hessian with the smallest eigenvalue, the validity of which is unclear when the Hessian is not full rank. Kleinberg et al. (2018) assumes that (convolving with) the noise in SGD makes the landscape one-point strongly convex, which implies that the loss landscape before the convolution is already close to a strongly convex landscape. Another commonly assumed condition is that the loss-landscape satisfies the Lojasiewicz condition, which is non-convex but implies the unrealistic condition that there is no local minimum except the global minimum (Karimi et al., 2020; Wojtowytsch, 2021a; Vaswani et al., 2019), which is not sufficient to understand the complicated dynamics that often happen in a setting with many minima. In section 6.5, we show that these assumptions do not hold even for the simplest kind of non-linear neural network with 2 layers and 1 hidden neuron. The central message of our work is that, without making model and task-dependent assumptions regarding the SGD noise, the behavior of the SGD algorithm may be arbitrary and independent of the underlying landscape.

4 A Warm-up Example

This section studies a special example of the main results of this work. While the setting of this example is restricted, it captures the essential features and mechanisms of SGD that we will utilize to prove the main results. Consider the following loss function:

$$\hat{L}(w) = \frac{x}{2}w^2, \quad (4)$$

where $x, w \in \mathbb{R}$ and x is drawn from an underlying distribution $p(x)$ at every time-step. We let $\mathbb{E}[x] = a$ and assume that $\text{Var}[x] = \sigma^2$ is finite. The stationary point of this loss function is $w = 0$. When $a > 0$, the underlying (deterministic) landscape is a local minimum; the $a > 0$ case is now well understood in the discrete-time limit and when the underlying noise is state-dependent (Liu et al., 2021). When $a < 0$, the point $w = 0$ is a local maximum, and the underlying dynamics need to escape from $w = 0$ to infinity, and our goal is to understand the behavior of SGD in this case.

The following proposition and proof show that there exists some seemingly benign data distribution $p(x)$ (zero-mean and bounded) such that SGD cannot escape from the local maximum when the learning rate is set to be 1.

Proposition 1. *Let $\lambda = 1$ and $a < 0$ and $p(x)$ be the distribution such that $x = 1$ and $x = -1 + a$ with equal probability. Then, w converges to $w = 0$ with probability 1 with the SGD algorithm, independent of the initialization.*

Proof. By the definition of the SGD algorithm, we have

$$w_{t+1} = \begin{cases} 0 & \text{with probability } 0.5; \\ (2-a)w_t & \text{otherwise.} \end{cases} \quad (5)$$

Therefore, after t time steps, w_t has at most 2^{-t} probability of being non-zero. For infinite t , $w_t = 0$ with probability 1. \square

Despite the simplicity of this example, it already contains a few surprising points. First of all, it suggests that one cannot use the expected value of w to study the escape problem of SGD. The expectation of w_t in this example is

$$\mathbb{E}_x[w_t] = (1-a/2)\mathbb{E}_x[w_{t-1}] = (1-a/2)^t w_0 = w_0 e^{\ln(1-a/2)t}, \quad (6)$$

which is an exponentially fast escape from any initialization w_0 for $a < 0$. In fact, $\ln(1-a)$ is exactly the escape time scale of the GD algorithm. This is counter-intuitive: *SGD will converge to the local maximum with probability 1, even if its expected value escapes the local maximum exponentially fast.*

Alternatively, one might also hope to use the expected loss or the norm $\mathbb{E}_{w_t}[L(w_t)] \sim \|w_t\|_2^2$ as the metric of escape, but it is not hard to see that it suffers the same problem. At time t , because $w_t = 0$ with probability $1/(1-2^{-t})$ and $w_t = (2-a)^t w_0$ with probability 2^{-t} , we have $\mathbb{E}[L(w_t)] \propto w_0^2 e^{2t \ln \frac{2-a}{\sqrt{2}}}$, which also predicts an exponentially fast escape. Again, this fails to reflect the fact that SGD has only a vanishingly small probability of escaping the constructed local maximum. Statistically speaking, the norms of w_t fail to be good metrics to measure the escape rate because these metrics are not robust against outliers. In our example, there is only 2^{-t} probability for SGD to escape the local minimum, yet the speed at which this outlier escapes the maximum outweighs the decay in its probability through time, thus contributing more to the expected norm than any other events. In short, this example also shows the difficulty and subtlety of dealing with the escape problem. In essence, the results in the rest of this work are extensions of this special case to less restrictive settings.

5 Main Results

In this section, we present 4 main theoretical results and propose one conjecture regarding SGD. Our main results are mathematical constructions that respectively show that (1) SGD may converge to a local

maximum; (2) SGD may escape a saddle point arbitrarily slowly; (3) SGD may prefer sharp minimum over the flat ones; and (4) AMSGrad may converge to a local maximum. Numerically, we show that these results are relevant for a minimal example involving a neural network, where the assumptions regarding SGD are violated (Section 6.5).

5.1 SGD May Converge to a Local Maximum

We show that there exist cases where SGD may fail to escape saddle points, while GD can successfully escape; this contradicts the suggestions in Kleinberg et al. (2018) that SGD always escapes local minimum faster than GD. It is appropriate to begin with the definition of a saddle point.

Definition 2. *w is said to be a stationary point of $L(w)$ if $\nabla_w L(w) = 0$. w is a minimum of L if for all w' in a sufficiently small neighborhood of w such that $L(w') \geq L(w)$. w is said to be a saddle point if w is a stationary point but not a local minimum.*

This definition of saddle point agrees with the common definition in the literature (Daneshmand et al., 2018). The following proposition explicitly constructs an example in which SGD cannot escape the local minimum.

Proposition 2. *Let Eq. 4 be the loss function. Let $\lambda > 0$, $w_0 \neq 0$, and $p(x) = \frac{1}{2}\delta(x-1) + \frac{1}{2}\delta(x+1-a)$; then SGD converges to the local maximum in probability if*

$$\frac{a}{a-1} < \lambda < \frac{a - \sqrt{a^2 - 8a + 8}}{2(a-1)}. \quad (7)$$

Proof Sketch. We first show that $\frac{1}{\sqrt{t}} \ln |w_t/w_0|$ obeys a normal distribution as $t \rightarrow \infty$. This allows us to deduce the accumulative distribution function (c.d.f.) of w as $t \rightarrow \infty$. The c.d.f. has an bifurcative dependence on the sign of $\mu := \mathbb{E}[\ln |1 - \lambda x|]$. When $\mu < 0$, the distribution of w_t converges to 0 in probability. See Section D.1 for the detailed proof. \square

Remark. *One can also make a straightforward extension of the above example to the case when $w = \mathbf{w} \in \mathbb{R}^d$ and $d > 1$, i.e., when \mathbf{w} is of high (but finite) dimension. In this case, let H denote the Hessian matrix at $\mathbf{w} = \mathbf{0}$. One can first diagonalize H and then show that there exists a critical eigenvalue $l_c(\lambda)$ such that for all subspaces H with eigenvalue $l \leq l_c$, \mathbf{w} will be attracted towards $\mathbf{0}$, and for all $l > l_c(\lambda)$ subspaces, \mathbf{w} will escape. If l_c is larger than all eigenvalues of H , then \mathbf{w} will never escape in all subspaces.*

Note that (also see Figure 3) there are three different regimes/phases for this simple escaping problem. The escape regime $\lambda > \frac{a - \sqrt{a^2 - 8a + 8}}{2(a-1)}$ is also present when $a > 0$; it means that in this regime, SGD will also escape the local minimum. This regime is not present if we perform a continuous-time analysis (Section C); this shows that this region is due to the instability of the *discrete-time* SGD algorithm. This kind of escaping is undesirable because, in this regime, the local gradient cannot provide any guidance for minimizing the loss. The region $\frac{a}{a-1} < \lambda < \frac{a - \sqrt{a^2 - 8a + 8}}{2(a-1)}$ is the trapped regime. This is due to the special structure of the minibatch noise – SGD will not be trapped if the noise is not position dependent. The small learning rate regime $\lambda < \frac{a}{a-1}$ is the successful escape regime because the SGD noise is of order λ^2 and becomes negligible at a small λ Liu et al. (2021).

5.2 SGD May Escape Saddle Points Arbitrarily Slowly

In the previous section, we have shown that for a fixed learning rate, one can adversarially construct a loss function such that the SGD algorithm converges to a local maximum. In this section, we show that, even if one can tune the learning rate at will, there exists loss landscapes where SGD can take an arbitrarily long time to escape, no matter how one chooses the learning rate. We begin by defining the escape rate.

Definition 3. *The asymptotic average escape rate of w at learning rate λ , $\gamma(\lambda)$, is defined as $\gamma := \lim_{t \rightarrow \infty} \frac{1}{t} \mathbb{E}[\ln |w_t|]$. The optimal escape rate is defined as $\gamma^* := \sup_{\lambda} \gamma(\lambda)$.*

Remark. Note that the definition above can be written as

$$\gamma = \lim_{t \rightarrow \infty} \left\{ \frac{1}{t} \mathbb{E}[|w_0|] + \frac{1}{t} \sum_{i=1}^t \mathbb{E} \left[\ln \left| \frac{w_i}{w_{i-1}} \right| \right] \right\} \approx \frac{1}{\tau} \sum_{i=1}^{\tau} \mathbb{E} \left[\ln \left| \frac{w_i}{w_{i-1}} \right| \right] \quad (8)$$

for a large τ . This alternative definition provides a way to estimate the escape rate during a finite time. Also, the readers familiar with the theory of dynamical systems will immediately notice this definition mirrors the definition of the Lyapunov exponent in the study of deterministic chaos (Schuster and Just, 2006; Lyapunov, 1992). In a sense, this definition can be seen as a generalization of the Lyapunov exponent to a probabilistic setting. We note that this definition of escape rate differentiates this work from the standard literature on escaping saddle points, where the focus is on the time scale it takes to reach a local minimum when saddle points exist (Ge et al., 2015; Daneshmand et al., 2018; Jin et al., 2017), while our definition focuses on the time scale of escaping a specified saddle point. These two time scales might be vastly different. For example, when the loss function is the cross-entropy loss, the global minimum is never reachable, yet escaping saddle points should be important and happen at a reasonable time. This definition is, therefore, more realistic and natural for studying escaping saddle points.

Escape can be achieved by setting the learning rate to be arbitrarily large; however, this is not possible in practice because the learning rate of SGD is inherently associated with the stability of learning (Ziyin et al., 2021), and λ usually has to be much smaller than 1.

Theorem 1. Assuming that $\lambda \leq 1$, there exist a differentiable loss function such that the SGD algorithm escapes the saddle point arbitrarily slowly, i.e., for any $\epsilon > 0$, there exists loss function such that $\sup_{\lambda} \gamma(\lambda) < \epsilon$.

Proof. An explicit construction is given by Proposition 3. \square

Proposition 3. Let the loss function be Eq. (4) and $p(x) \sim \frac{1}{2}\delta(x-1) + \frac{1}{2}\delta(x-a+1)$. Then $\gamma^* = \ln \frac{2-a}{2\sqrt{1-a}}$, and, for any $\epsilon > 0$, $\gamma^* < \epsilon$ if $|a| \leq 2 \left| -e^\epsilon \sqrt{e^{2\epsilon} - 1} - e^{2\epsilon} + 1 \right|$.

Intuitively, one expects escaping to be easier as we increase the learning rate (Kleinberg et al., 2018), and that the escape rate should monotonically increase as we increase the learning rate. This example conveys the surprising message that the escaping efficiency is not monotonically increasing as the learning rate increase. For this example, the escape rate first decrease and starts to increase only when λ is quite large. This example also shows the subtlety in the escaping problem. On the one hand, one needs to avoid a too large step size to avoid training instability. On the other hand, one cannot use a too small learning rate because a small learning rate also makes optimization slow. This interesting example suggests that there must be a tradeoff between learning speed and learning stability and that a general theory for finding the best learning rate that achieves the best tradeoff may be constructible; however, this tradeoff problem is a sufficiently complex problem on its own and is beyond the scope of the present work.

5.3 SGD May Prefer Sharper Minima

Modern deep neural networks are often overparametrized and capable of memorizing all the training data points quite easily. This means that the traditional metrics such as Rademacher complexity cannot be used to guarantee the generalization capability of SGD (Zhang et al., 2017). Nevertheless, neural networks are found to generalize surprisingly well. This leads to the hypothesis that SGD, the main training algorithm of neural networks, contains some implicit regularization effect such that it biases the neural network towards simpler solutions (Neyshabur et al., 2017; Soudry et al., 2018). One way through which SGD may help generalization is the hypothesized mechanism that SGD selects flat minima over the sharp ones (Hochreiter and Schmidhuber, 1997; Meng et al., 2020; Xie et al., 2021; Liu et al., 2021; Mori et al., 2021; Smith and Le, 2018; Wojtowysch, 2021b). In this work, we show that this may not be the case because the dynamics and convergence of SGD crucially depend on the underlying mini-batch noise, while the sharpness of the landscape is independent of the noise. Before introducing the results, let us first define the sharpness of a local minimum.

Definition 4. Let $w = w^*$ be a local minimum of the loss function $L(w)$; the sharpness $s(w^*)$ of local minimum w^* is defined as $s(w^*) := \text{Tr}[\nabla_w^2 L(w^*)]$. We say that a minimum w_1^* is sharper than w_2^* if and only if $s(w_1^*) > s(w_2^*)$.

In this definition, the sharpness is the trace of the Hessian of the quadratic approximation to the local minimum. Other possible definitions such as the determinant of the Hessian are essentially similar to this definition (Dinh et al., 2017).

For an explicit construction, consider the following objective on a 2-dimensional landscape:

$$\hat{L}(w_1, w_2) = \frac{1}{2} [-(w_1 - w_2)^2 - (w_1 + w_2)^2 + (w_1 - w_2)^4 + (w_1 + w_2)^4 - 2aw_2^2 + xbw_1^2]. \quad (9)$$

for $a, b > 0$ and $p(x) = \frac{1}{2}\delta(x-1) + \frac{1}{2}\delta(x+1)$. The diagonal terms of the Hessian of the loss function is given by

$$\begin{cases} \frac{\partial^2}{\partial w_1^2} \hat{L}(w_1, w_2) = -2 + 12w_1^2 + 12w_2^2 \\ \frac{\partial^2}{\partial w_2^2} \hat{L}(w_1, w_2) = -2 - 2a + 12w_1^2 + 12w_2^2. \end{cases} \quad (10)$$

There are four local minima in total for this loss function. These minima and their sharpnesses are

$$\begin{cases} (w_1, w_2) = (\pm \frac{1}{\sqrt{2}}, 0) & \text{with } s = 4; \\ (w_1, w_2) = (0, \pm \sqrt{\frac{1+a}{2}}) & \text{with } s = 4 + 4a. \end{cases} \quad (11)$$

We see that for positive a , the minima at $(0, \pm \sqrt{\frac{1+a}{2}})$ are sharper than the other two minima. We show that SGD will converge to these sharper minima. For this example, we assume that w_1 and w_2 are bounded because, if initialized sufficiently far from origin, the fourth-order term will cause divergence.

Proposition 4. Let the loss function be Eq. (9), $|w_1| \leq 1$ and $|w_2| \leq 1$. For any $\lambda < c$ for some constant $c = O(1)$, there exists some b such that if SGD converges in probability, it will converge to the sharper minimum at $(w_1, w_2) = (0, \pm \sqrt{\frac{1+a}{2}})$.

Remark. In this example, the noise is not full-rank, which is often the case in a deep learning setting for overparametrized networks (Wojtowysch, 2021a). For example, when weight decay is used, the Hessian of the loss function should be full rank, while the rank of the noise covariance should be proportional to the inherent dimension of the data points, which is in general much smaller than the dimension of the Hessian in deep learning (Ansuini et al., 2019).

The proof is technical and delayed to the appendix Section D.3. In fact, it has been controversial whether finding a shallow minimum can help generalization. For example, Dinh et al. (2017) shows that, for every flat minimum of a ReLU-based net, there exists a minimum that is arbitrarily sharper and generalizes as well. However, this work does not rule out the possibility that conditioning on using gradient-based optimization, the performance of the sharper minima that gradient descent finds is worse than the performance of the flatter minima. If this assumption is valid, then biasing gradient descent towards flatter minima can indeed help, and the stochasticity of SGD has been hypothesized to help in this regard. However, our construction shows that SGD, on its own, may be incapable of helping to converge to a flatter minimum. At least some other assumptions need to be invoked to show that SGD may help. For example, the definition of the neural networks may endow these models with a special kind of Hessian and noise structure such that when combined with SGD, results in a miraculous generalization behavior. However, to the best of our knowledge, no previous work have pursued this direction, and future study in this direction may be fruitful.

Moreover, it is worth commenting that, in the particular example we studied, SGD will converge to the local minimum at $(0, \pm \sqrt{\frac{1+a}{2}})$ independent of its sharpness due to the special noise we constructed. This fact hints at the crucial role of noise in SGD optimization. In fact, if we allow arbitrary space dependent noise, it might be the case that SGD may converge to arbitrary distribution that is independent of the underlying landscape; we briefly discuss this possibility in the form of a conjecture in Section D.5.

5.4 Non-Convergence of Adaptive Gradients

Adam (Kingma and Ba, 2014) and its closely related variants such as RMSProp (Tieleman and Hinton, 2012) have been shown to converge to a local maximum even for some simple convex loss landscapes (Reddi et al., 2018a). The proposed fix, named AMSGrad, takes the maximum of all the previous preconditioners in Adam. This section shows that AMSGrad may also converge to a local maximum even in simple non-convex settings. Let $x_t \sim p(x)$ and $\hat{g}_t = \nabla \ell(x_t, w_{t-1})$, the Adam takes the form by Figure 2, where $v_0 = 0$. We have removed the numerical smoothing constant ϵ from the denominator, which causes no problem if w_0 is initialized away from 0. Here, β_1 is the momentum hyperparameter. v_t is called the preconditioner, and β_2 is the associated hyperparameter. The standard value for β_1 is 0.9 and β_2 is 0.999. In our theory, we only consider the case when $\beta_1 = 0$. In the experiment section, we show that similar problem exists when $\beta_1 > 0$ (but with some additional interesting findings). Intuitively, this is easy to understand because AMSGrad behaves like SGD asymptotically, so we only have to wait for long enough, and the results in previous sections would apply. The construction below follows this intuition.

$$m_t = \beta_1 m_{t-1} + (1 - \beta_1) \hat{g}_t; \quad (12)$$

$$v_t = \beta_2 v_{t-1} + (1 - \beta_2) \hat{g}_t^2; \quad (13)$$

$$\hat{v}_t = \max(\hat{v}_{t-1}, v_t); \quad (14)$$

$$w_t = w_{t-1} - \frac{\lambda}{\sqrt{\hat{v}_t}} m_t. \quad (15)$$

Figure 2: AMSGrad Algorithm.

Proposition 5. *Let $w_t \in [-1, 1]$, and $w_0 \neq 0$. For fixed $\lambda < 1$ and the loss function in Eq. (4) there exists $a < 0$ such that the AMSGrad algorithm converges in probability to a local maximum.*

Remark. *The proof is given in Section D.4. It is interesting to note that the example we constructed is similar to the original construction in Reddi et al. (2018a) that shows that Adam converges to a maximum while AMSGrad. In their example (with some rescaling), the gradient is a random variable*

$$\hat{g}_t = \begin{cases} 1 & \text{with probability } q \approx 1; \\ c_0 < 0 & \text{with probability } 1 - q \ll 1; \end{cases} \quad (16)$$

such that the expected gradient is negative, and Adam is shown to converge to the direction opposite the gradient descent (therefore to a maximum). In our example, the gradient is (roughly)

$$\hat{g}_t = \begin{cases} w_{t-1} & \text{with probability } 1/2; \\ -(1+a)w_{t-1} & \text{with probability } 1/2; \end{cases} \quad (17)$$

and the expected gradient also increases $|w_t|$, However, AMSGrad is shown to decrease $|w_t|$ in probability. Therefore, our example can be seen as a minimal generalization of the Reddi et al. (2018a) example to a non-convex setting.

There is no reason to expect an algorithm that converges in a convex setting to converge in a general non-convex setting, and there is even less reason to expect convergence in a stochastic setting. In fact, there has not been any convincing evidence that Adam fails badly in a practical setting (Choi et al., 2020). This example also raises the question of whether convergence is really needed for learning. In terms of biology, the human brain is constantly adapting and shows no sign of convergence throughout its lifetime (Kandel et al., 2000); the brains that show little or no sign of adaptation often suffer from severe cognitive diseases (Pittenger and Duman, 2008). We do not argue that convergence is not important for machine learning, but that we need to rethink the role of mathematical convergence if general artificial intelligence is to be achieved.

6 Experimental Illustrations

In this section, we perform experiments to illustrate and visualize the examples studied in this work.

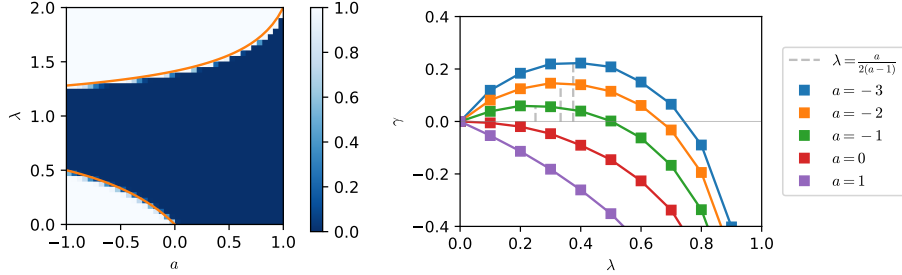


Figure 3: **Left:** Escape probability as a function of a and λ . The parameters space is divided into an absorbing phase where w is attracted to the local maximum (in **dark blue**) and an active phase where w escapes the two central bins successfully (in white). The binning is the same as in Figure 1. **Right:** Escape rate γ as a function of learning rate λ with quadratic loss landscape, obtained by simulations. We note that the escape-rate analysis yields results which are compatible with the phase diagram.

6.1 SGD Converges to a Local Maximum

Numerical results are obtained for the setting described in section 5.1. See Figure 1-Left. The loss landscape is defined by $L(w) = \frac{1}{2}xw^2$, and $p(x) = \frac{1}{2}\delta(x-1) + \frac{1}{2}\delta(x+1-a)$. In this numerical example, we set $\lambda = 0.8$ and $a = -1$, and the histogram is plotted with 2000 independent runs. We see that the distribution converges to the local maximum at $w = 0$ as the theory predicts. For better qualitative understanding, we also plot the empirical phase diagram of this setting in Figure 3. We perform numerical evaluations for different combinations of a and λ on a $a-\lambda$ plane, and for each combination, we plot the percentage of w that escapes the two central bins (white is 100% and **dark blue** is 0%). For completeness, we also plot the case when $a > 0$, i.e., when the critical point at $w = 0$ is a local minimum. The orange line shows where the phase transition is expected to happen according to Eq. (7). The fact that the orange line agrees exactly with the empirical phase transition line confirms our theory.

We also numerically study a closely related fourth-order loss landscape, defined as $\hat{L}(w) = \frac{1}{2}xw^2 + \frac{1}{4}w^4$, where the distribution $p(x)$ is the same as before. See Figure 1-Right. The expected loss $L(w)$ has two local minima located as $w = \pm\sqrt{a}$. We are interested in finding whether SGD can converge to these two points successfully; note that, without the fourth-order term, this loss is the same as the quadratic loss we studied. See Figure 1-Right. As before, $a = -1$ and $\lambda = 0.8$. We see that the distribution of w also concentrates towards the local maximum after training, and no w is found to converge to the two local minimum even if a significant proportion of w is initialized close to these two minima. A phase diagram analysis is given in the Section A.1.

6.2 Escape Rate Experiments

This sections illustrates the slow escape problem studied in Section 5.2. See Figure 3-Right. γ is calculated by averaging the first 50 time steps across 2000 independent runs. We see that, as our theory predicts, as $|a|$ gets closer to 0, the optimal escape rate decreases towards 0. This implies that there exists landscape such that SGD is arbitrarily slow at learning, independent of parameter tuning. One additional observation is that the optimal learning rate is neither too large or too small, i.e., there seems to be a tradeoff between the escape speed and escape probability (and also between the speed and stability). See also the discussion at the end of Section 5.2.

6.3 Convergence to the Sharper Minimum

We use the same 2-dimensional loss landscape defined in Section 5.3. The experiment is run with 2000 independent simulations and learning rate $\lambda = 0.05$. See Figure 4, where we overlap the underlying landscape with the empirical distribution (the heat map). We see that, even though the initialization overlaps significantly with the local flatter minimum, all points converge to the sharper minimum, as the theorem proves.

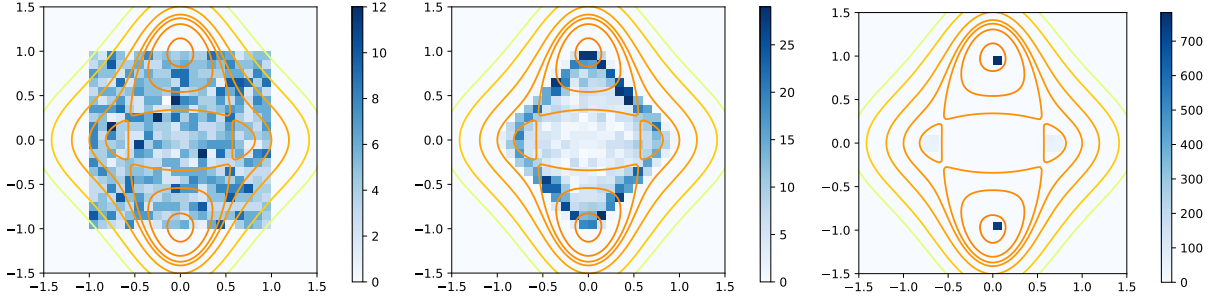


Figure 4: Evolution of the distribution of w in a landscape where two flat minima and two sharp minima exist. As Proposition 4 shows, the model parameters converge to the sharper minima even if initialized in the flat minimum. **Left:** Initialization. **Mid:** step 2. **Right:** step 10000.

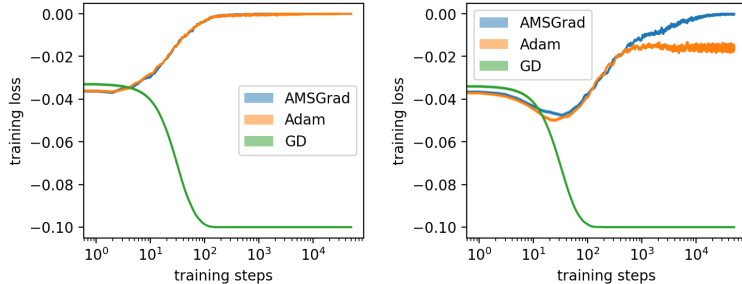


Figure 5: Divergence of AMSGrad. AMSGrad diverges to the local maximum with or without momentum. Our result shows that AMSGrad is always attracted to the local maximum, while Adam has the potential of escaping the local maximum with momentum. **Left:** without momentum. **Right:** with momentum.

6.4 Non-Convergence of AMSGrad

In this section, we illustrate the example of convergence behavior of AMSGrad; for reference, we also plot the behavior of Adam and gradient descent for this example. See Figure 5. The experiment is the average over 2000 runs, each with 5×10^4 steps. The uncertainty is reflected by the shaded region (almost invisibly small). The loss function is the same as discussed in Section 5.4 with $a = -0.1$. For illustration purposes, we set $\lambda = 0.2$ and $\beta_2 = 0.999$ for both Adam and AMSGrad. When momentum is used, we set $\beta_1 = 0.9$. We also show the convergence of GD for comparison, with a learning rate of 0.01. Without momentum, both Adam and AMSGrad converges to the local maximum with almost the same speed. When momentum is added, AMSGrad still converges to the local maximum. Surprisingly, Adam is no longer attracted to the local maximum but also remains away from the local minimum. This suggests that Adam, with momentum, might have a better capability of escaping saddle points than AMSGrad and might be preferable to AMSGrad in a non-convex setting (and realistic problems are likely to be non-convex).

6.5 A Neural Network Example

Now, we consider a minimal neural network example to illustrate our point. The network is defined as $f(x) = w_2 \sigma(w_1 x)$, where $w_1, w_2 \in \mathbb{R}$. σ is the non-linearity, and we let $\sigma(x) = x^2$ as a minimal example. This is the simplest kind of non-linear feedforward network one can construct (2 layer with a single hidden neuron). We also pick a minimal dataset with a single data point: $x = 1$ with probability 1 and $y \in \{-1, 2\}$, each with probability 0.5, i.e., the label has a degree of inherent uncertainty, which is often the case in real problems. We use mean squared error (MSE) as the loss function. Therefore, the expected loss is

$$L(w_1, w_2) = \frac{1}{2}(w_2 w_1^2 + 1)^2 + \frac{1}{2}(w_2 w_1^2 - 2)^2. \quad (18)$$

The global minimum $L^* = 2.25$ is degenerate, and is achieved when $w_1 = \sqrt{1/2w_2}$. Crucially, the set $\{(w_1, w_2) | w_1 = 0, w_2 \geq 0\}$ contains all the saddle points with $L = 2.5$. Despite the simplicity of this example,

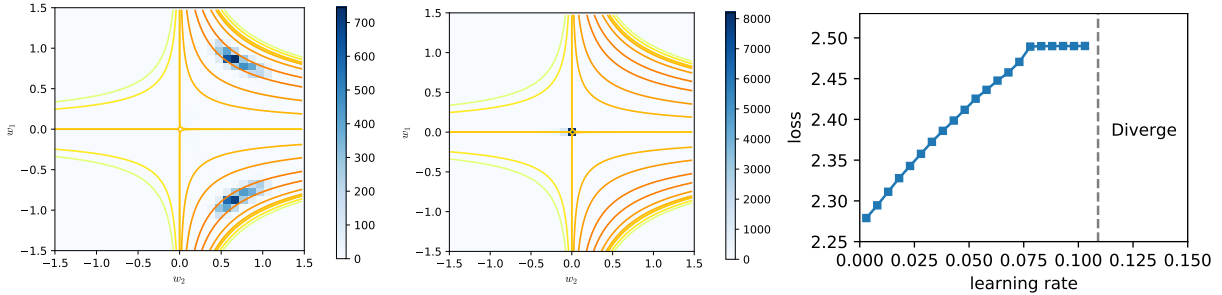


Figure 6: The distribution of parameters and loss for a two-layer one-neuron neural network. **Left:** $\lambda = 0.001$ at step 10000. **Mid:** $\lambda = 0.1$ at step 10000. **Right:** Average loss in equilibrium as a function of learning rate. The loss function diverges for learning rate larger than 0.108.

it contains many essential features in a realistic problem: (1) inherent uncertainty in the data; (2) a non-linear neural network with more than 1 layer; (3) the minimum is degenerate and has zero eigenvalues in the Hessian. Moreover, the advantage of this example is that it contains only two parameters and we can illustrate it simply.

More importantly, most previous works on the convergence or escaping behavior of SGD are inapplicable to this example. One dominant assumption is the ρ -Hessian Lipschitz property (Jin et al., 2017; Ge et al., 2015), which does not hold for any deep neural network in general and for this example in particular. Another common assumption is the PL condition (Karimi et al., 2020; Wojtowytsch, 2021a; Vaswani et al., 2019), which does not apply due to the existence of the saddle point. One recent assumption is that the loss function is 1-point convex for all points (Kleinberg et al., 2018), which is also ruled because $(0,0)$ is not 1-point strongly convex. Another relevant assumption is the correlated negative curvature assumption, which also does not hold for $(0,0)$. We show in Section A.3 in detail why these conditions are violated.

See Figure 6 for the experiment with this example. w_1 is initialized uniformly in $[-1, 1]$; w_2 is initialized uniformly in $[0, 1]$ to be closer to the global minimum and away from the saddle point (standard initialization such as initializing in $[-1, 1]$ does not change the conclusion). The left figure shows the stationary distribution of the model parameter at a small learning rate ($\lambda = 0.001$). All the parameters are located in the global minimum valley as expected. In contrast, when the learning rate is large ($\lambda = 0.1$), the central figure shows that all models (1000 independent runs) converge to the saddle point at $(0,0)$. The right figure investigates this change more systematically and shows the change in the average stationary training loss of the models as we increase the learning rate from 0.001 to 0.15. We see that for a small learning rate, the training loss is close to that of the global minima ($L = 2.25$), and for a significant range of large learning rates, the model invariably converges to a saddle point. One additional interesting observation is that the model diverges at $\lambda \approx 0.11$, and there is almost no sign of such divergence (such as increased fluctuation or a power-law behavior) when the learning rate is close to the divergent threshold. This example shows the relevance of our results to the study of neural networks. In fact, it has often been noticed that at convergence, many large-scale neural networks in realistic tasks exhibit negative eigenvalues in the Hessian (Alain et al., 2019; Granzio et al., 2019). The existence of large eigenvalues at a late time either suggests that the algorithm has yet to escape or that it has indeed been attracted to such saddle points; if the latter is true, then our work offers an explanation. The emergence of negative eigenvalues at the end of training serves as indirect evidence that our result may be relevant for larger neural networks.

7 Concluding Remarks

We have shown that many unexpected phenomena may happen for SGD when we relax the strong assumptions. The problems we found are shown to be directly relevant for a minimal learning example involving a neural network. Despite the minimality of the setting, we have shown that the majority of theoretical works are based on assumptions that this example violates. The limitation of this work is obvious: the focus on direct proofs and illustrative analyses of SGD has restricted us to elementary loss functions, and it is unclear to what extent these results carry over to more realistic problems involving more wider and deeper

architectures. If the result partially applies to large-scale neural networks, then our result becomes a negative result regarding using SGD and adaptive gradient and should motivate for developing more advanced methods for stochastic optimization. If the result does not carry over, one important future problem is to figure out why the studied scenarios deviates far from the settings in deep learning, and this can only be achieved if we have a solid understanding of the actual shape, strength, and structure of the SGD noise for such neural networks, which we believe will be a crucial theoretical problem in the foreseeable future. This work should serve as a cautionary note to speculations about different kinds of advantages of SGD. Also, we comment that when the dataset size is finite, convergence to the global minimum is necessarily associated with overfitting; it might not be an undesirable thing to not converge to the global minimum. For example, it is well possible for “benign” saddle points (with good generalization properties and non-zero training loss) to exist, and one might design special algorithms to avoid overfitting by making such benign saddle points attractive. Lastly, our sincere hope is that this work may bring more attention to the field of stochastic optimization research in the context of deep learning.

References

- Alain, G., Roux, N. L., and Manzagol, P.-A. (2019). Negative eigenvalues of the hessian in deep neural networks. *arXiv preprint arXiv:1902.02366*.
- Allen-Zhu, Z., Li, Y., and Song, Z. (2018). A convergence theory for deep learning via over-parameterization. *arXiv preprint arXiv:1811.03962*.
- Ansuini, A., Laio, A., Macke, J. H., and Zoccolan, D. (2019). Intrinsic dimension of data representations in deep neural networks.
- Bottou, L. (2012). Stochastic gradient descent tricks. In *Neural networks: Tricks of the trade*, pages 421–436. Springer.
- Choi, D., Shallue, C. J., Nado, Z., Lee, J., Maddison, C. J., and Dahl, G. E. (2020). On empirical comparisons of optimizers for deep learning.
- Daneshmand, H., Kohler, J., Lucchi, A., and Hofmann, T. (2018). Escaping saddles with stochastic gradients. In *International Conference on Machine Learning*, pages 1155–1164. PMLR.
- Dinh, L., Pascanu, R., Bengio, S., and Bengio, Y. (2017). Sharp minima can generalize for deep nets. In *International Conference on Machine Learning*, pages 1019–1028. PMLR.
- Dinh, L., Pascanu, R., Bengio, S., and Bengio, Y. (2017). Sharp Minima Can Generalize For Deep Nets. *ArXiv e-prints*.
- Du, S. S., Jin, C., Lee, J. D., Jordan, M. I., Póczos, B., and Singh, A. (2017). Gradient descent can take exponential time to escape saddle points. *arXiv preprint arXiv:1705.10412*.
- Du, S. S., Zhai, X., Póczos, B., and Singh, A. (2018). Gradient descent provably optimizes over-parameterized neural networks. *arXiv preprint arXiv:1810.02054*.
- Feng, Y. and Tu, Y. (2021). The inverse variance–flatness relation in stochastic gradient descent is critical for finding flat minima. *Proceedings of the National Academy of Sciences*, 118(9).
- Ge, R., Huang, F., Jin, C., and Yuan, Y. (2015). Escaping from saddle points—online stochastic gradient for tensor decomposition. In *Conference on learning theory*, pages 797–842. PMLR.
- Gower, R., Sebbouh, O., and Loizou, N. (2021). Sgd for structured nonconvex functions: Learning rates, minibatching and interpolation. In *International Conference on Artificial Intelligence and Statistics*, pages 1315–1323. PMLR.

- Granziol, D., Garipov, T., Zohren, S., Vetrov, D., Roberts, S., and Wilson, A. G. (2019). The deep learning limit: are negative neural network eigenvalues just noise? In *ICML 2019 Workshop on Theoretical Physics for Deep Learning*.
- Gurbuzbalaban, M., Simsekli, U., and Zhu, L. (2021). The heavy-tail phenomenon in sgd. In *International Conference on Machine Learning*, pages 3964–3975. PMLR.
- Hochreiter, S. and Schmidhuber, J. (1997). Flat minima. *Neural Computation*, 9(1):1–42.
- Hodgkinson, L. and Mahoney, M. W. (2020). Multiplicative noise and heavy tails in stochastic optimization. *arXiv preprint arXiv:2006.06293*.
- Hoffer, E., Hubara, I., and Soudry, D. (2017). Train longer, generalize better: closing the generalization gap in large batch training of neural networks. In *Proceedings of the 31st International Conference on Neural Information Processing Systems*, pages 1729–1739.
- Jastrzebski, S., Kenton, Z., Arpit, D., Ballas, N., Fischer, A., Bengio, Y., and Storkey, A. (2017). Three factors influencing minima in sgd. *arXiv preprint arXiv:1711.04623*.
- Jin, C., Ge, R., Netrapalli, P., Kakade, S. M., and Jordan, M. I. (2017). How to escape saddle points efficiently. In *International Conference on Machine Learning*, pages 1724–1732. PMLR.
- Kandel, E. R., Schwartz, J. H., Jessell, T. M., Siegelbaum, S., Hudspeth, A. J., and Mack, S. (2000). *Principles of neural science*, volume 4. McGraw-hill New York.
- Karimi, H., Nutini, J., and Schmidt, M. (2020). Linear convergence of gradient and proximal-gradient methods under the polyak-lojasiewicz condition.
- Kingma, D. P. and Ba, J. (2014). Adam: A method for stochastic optimization. *CoRR*, abs/1412.6980.
- Kleinberg, B., Li, Y., and Yuan, Y. (2018). An alternative view: When does sgd escape local minima? In *International Conference on Machine Learning*, pages 2698–2707. PMLR.
- Lee, J. D., Simchowitz, M., Jordan, M. I., and Recht, B. (2016). Gradient descent only converges to minimizers. In *Conference on learning theory*, pages 1246–1257. PMLR.
- Li, Z., Malladi, S., and Arora, S. (2021). On the validity of modeling sgd with stochastic differential equations (sdes). *arXiv preprint arXiv:2102.12470*.
- Liu, K., Ziyin, L., and Ueda, M. (2021). Noise and fluctuation of finite learning rate stochastic gradient descent.
- Lyapunov, A. M. (1992). The general problem of the stability of motion. *International journal of control*, 55(3):531–534.
- Mandt, S., Hoffman, M. D., and Blei, D. M. (2017). Stochastic gradient descent as approximate bayesian inference. *Journal of Machine Learning Research*, 18:1–35.
- May, R. (1976). Simple mathematical models with very complicated dynamics. *nature*. vol. 251, june. 10.
- Meng, Q., Gong, S., Chen, W., Ma, Z.-M., and Liu, T.-Y. (2020). Dynamic of stochastic gradient descent with state-dependent noise. *arXiv preprint arXiv:2006.13719*.
- Mori, T., Ziyin, L., Liu, K., and Ueda, M. (2021). Logarithmic landscape and power-law escape rate of sgd. *arXiv preprint arXiv:2105.09557*.
- Ndao, M. (2016). Convergence to equilibrium for fokker-planck equation with a general force field.
- Neyshabur, B., Tomioka, R., Salakhutdinov, R., and Srebro, N. (2017). Geometry of optimization and implicit regularization in deep learning. *arXiv preprint arXiv:1705.03071*.

- Pittenger, C. and Duman, R. S. (2008). Stress, depression, and neuroplasticity: a convergence of mechanisms. *Neuropsychopharmacology*, 33(1):88–109.
- Reddi, S., Kale, S., and Kumar, S. (2018a). On the convergence of adam and beyond. In *International Conference on Learning Representations*.
- Reddi, S., Zaheer, M., Sra, S., Póczos, B., Bach, F., Salakhutdinov, R., and Smola, A. (2018b). A generic approach for escaping saddle points. In *International conference on artificial intelligence and statistics*, pages 1233–1242. PMLR.
- Risken, H. (1996). Fokker-planck equation. In *The Fokker-Planck Equation*, pages 63–95. Springer.
- Schuster, H. G. and Just, W. (2006). *Deterministic chaos: an introduction*. John Wiley & Sons.
- Smith, S. L. and Le, Q. V. (2018). A bayesian perspective on generalization and stochastic gradient descent. In *International Conference on Learning Representations*.
- Soudry, D., Hoffer, E., Nacson, M. S., Gunasekar, S., and Srebro, N. (2018). The implicit bias of gradient descent on separable data. *The Journal of Machine Learning Research*, 19(1):2822–2878.
- Tieleman, T. and Hinton, G. (2012). Lecture 6.5—RmsProp: Divide the gradient by a running average of its recent magnitude. COURSE: Neural Networks for Machine Learning.
- Vaswani, S., Bach, F., and Schmidt, M. (2019). Fast and faster convergence of sgd for over-parameterized models and an accelerated perceptron. In *The 22nd International Conference on Artificial Intelligence and Statistics*, pages 1195–1204. PMLR.
- Welling, M. and Teh, Y. W. (2011). Bayesian learning via stochastic gradient langevin dynamics. In *Proceedings of the 28th international conference on machine learning (ICML-11)*, pages 681–688. Citeseer.
- Wojtowytsch, S. (2021a). Stochastic gradient descent with noise of machine learning type. part i: Discrete time analysis. *arXiv preprint arXiv:2105.01650*.
- Wojtowytsch, S. (2021b). Stochastic gradient descent with noise of machine learning type. part ii: Continuous time analysis. *arXiv preprint arXiv:2106.02588*.
- Wu, L., Zhu, Z., and E, W. (2017). Towards Understanding Generalization of Deep Learning: Perspective of Loss Landscapes. *ArXiv e-prints*.
- Xie, Z., Sato, I., and Sugiyama, M. (2021). A diffusion theory for deep learning dynamics: Stochastic gradient descent exponentially favors flat minima. In *International Conference on Learning Representations*.
- Xing, C., Arpit, D., Tsirigotis, C., and Bengio, Y. (2018). A walk with sgd. cite arxiv:1802.08770Comment: First two authors contributed equally.
- Zhang, C., Bengio, S., Hardt, M., Recht, B., and Vinyals, O. (2017). Understanding deep learning requires rethinking generalization.
- Zhang, C., Liao, Q., Rakhlin, A., Miranda, B., Golowich, N., and Poggio, T. (2018). Theory of deep learning iib: Optimization properties of sgd. *arXiv preprint arXiv:1801.02254*.
- Zhiyi, Z. and Ziyin, L. (2021). On the distributional properties of adaptive gradients. *arXiv preprint arXiv:2105.07222*.
- Zhu, Z., Wu, J., Yu, B., Wu, L., and Ma, J. (2019). The anisotropic noise in stochastic gradient descent: Its behavior of escaping from sharp minima and regularization effects. In *International Conference on Machine Learning*, pages 7654–7663. PMLR.
- Ziyin, L., Liu, K., Mori, T., and Ueda, M. (2021). On minibatch noise: Discrete-time sgd, overparametrization, and bayes. *arXiv preprint arXiv:2102.05375*.

Zou, D., Wu, J., Braverman, V., Gu, Q., and Kakade, S. M. (2021). Benign overfitting of constant-stepsize sgd for linear regression. *arXiv preprint arXiv:2103.12692*.

A Additional Experiments

A.1 Phase Diagram of the Fourth Order Loss Function

The fourth-order loss function is a more realistic loss function than the one we considered in Section 5.1. We also performed one experiment in the main text (See Figure 1). Here, we plot its phase diagram. We see that for this loss landscape also, there is some region such that for all λ , SGD converges to the local maximum. This loss landscape is very difficult to study in discrete time as it is known to lead to chaotic behavior at large step size (May, 1976). Therefore, we alternatively try to understand this landscape using continuous approximation. See Section C.

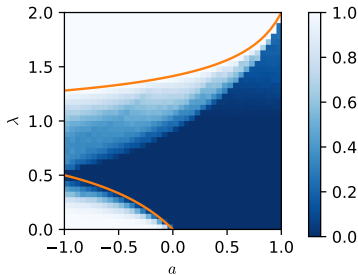


Figure 7: Escape probability from the local maximum as a function of a and λ with fourth order loss landscape. The parameters space is divided into an absorbing phase where w is attracted to the local maximum and an active phase where w escapes to infinity successfully. The orange line is the theoretical phase transition line for the quadratic loss function. We see that when λ is small, the line based on quadratic loss also gives good agreement with the fourth-order loss. This suggests that part of this result is universal and independent of the details of the loss function.

A.2 Estimating the Escape Rate

In the escape rate experiments, the empirical results are obtained from the proposed approximation in Eq. (8). Here, we show that it is valid. See Figure 8, where we plot the estimated γ as a function of the training step. We see that the estimated value converges within about 20 steps. We, therefore, estimate the escape rates at time step 100 in the main text.

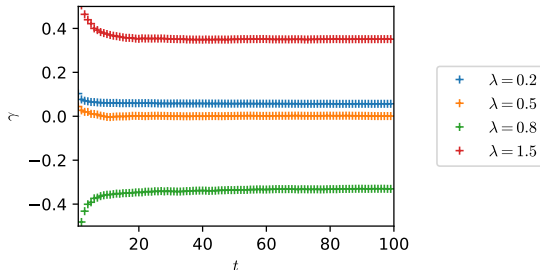


Figure 8: Escape rate γ as a function of time step t obtained when $a = -1$, showing that γ , defined in Equation (88), is indeed a well-defined quantity when t is large. γ becomes stable after roughly 40 steps.

A.3 Failure of Standard Assumption for the Neural Network Example

In this section, we show that the standard assumptions in the previous literature does not hold for the example studied in Section 6.5. One common assumption is that the loss function is ρ -Hessian Lipschitz.

Definition 5. A loss function L is said to be ρ -Hessian Lipschitz if, for some $\rho > 0$,

$$\forall \mathbf{w}, \mathbf{w}', \|\nabla^2 L(\mathbf{w}) - \nabla^2 L(\mathbf{w}')\| \leq \rho \|\mathbf{w} - \mathbf{w}'\|. \quad (19)$$

This certainly does not hold for the example we considered. Explicitly, let $w_2 = 0$, the Hessian $H(\mathbf{w})$ of the loss function is

$$H_{w_1, w_1} = H_{w_1, w_2} = H_{w_2, w_1} = 0, \quad (20)$$

and

$$H_{w_2, w_2} = -w_1^2. \quad (21)$$

Let $w_1 \rightarrow \infty$ violates the ρ -Hessian Lipschitz property.

Another common assumption for non-convex setting is the PL condition.

Definition 6. Let L^* be the value of L at the global minimum. A loss function L is said to satisfy the PL (Lojasiewicz) condition if

$$\forall \mathbf{w}, \|\nabla L(\mathbf{w})\|^2 \geq \mu(L(\mathbf{w}) - L^*), \quad (22)$$

for some $\mu > 0$.

This also does not hold due to the existence of the saddle point. Let $(w_1, w_2) = (0, 0)$. The gradient is zero, but the right hand side is greater than 0.

Recently, the correlated negative curvature assumption has been proposed to study the escaping behavior of SGD.

Definition 7. Let $\mathbf{v}_{\mathbf{w}}$ be the eigenvector of the minimum eigenvalue of the Hessian $H(\mathbf{w})$. L satisfies the correlated negative curvature assumption if, for some $\gamma > 0$,

$$\forall \mathbf{w}, \mathbb{E}_x[\langle \mathbf{v}_{\mathbf{w}}, \nabla L(x, \mathbf{w}) \rangle^2] > \gamma \quad (23)$$

where x is the data point.

This also does not hold. The point $(0, 0)$ violates this condition because $\nabla L(x, \mathbf{w}) = 0$ for all x at $(w_1, w_2) = (0, 0)$. In fact, it is exactly this point that violates this condition that the SGD converges to in this example.

Recently, the one point strongly convex assumption has been proposed to study the escaping behavior of SGD.

Definition 8. A loss function is said to satisfy the c -one point strongly convex condition with respect to \mathbf{w}^* for all gradient noise ϵ , $c > 0$, define $\mathbf{v} = \mathbf{w} - \lambda \nabla L(\mathbf{w})$, we have

$$\langle -\nabla \mathbb{E}_\epsilon L(\mathbf{v} - \lambda \mathbf{w}, \mathbf{w}^* - y) \rangle \geq c \|\mathbf{w}^* - \mathbf{v}\|_2^2, \quad (24)$$

where ϵ is the random noise caused by minibatch sampling.

This assumption is equivalent to that the loss landscape is strongly-convex after convoluting with the noise. This condition implies that there is only a single stationary point. However, this is not the case, consider any point with $w_1 = 0$ and $w_2 \leq 0$. These points have zero gradient for $w_1 \leq 0$ and so $\epsilon = 0$ with probability 1. Then, these points all have the same loss after the convolution:

$$\mathbb{E}[L(\mathbf{v} - \lambda \epsilon)] = L(\mathbf{v}), \quad (25)$$

which either imply that the landscape is not convex or that there is more than 1 stationary point, and so the system is not one point strongly convex.

B Additional Theoretical Concerns

B.1 Two Frequently Used Lemmas

We first prove the following lemma regarding the limiting distribution of $\ln |w_t|$.

Lemma 1. *Let the loss function be $\hat{L}(w) = \frac{1}{2}xw^2$, $x \sim p(x)$ such that $\text{Var}[x] = \sigma^2$ and $\mathbb{E}_x[x] = a < 0$ and that $p(x)$ is continuous in a δ -neighborhood of $x = 1$, and $w_0 \neq 0$. Then, for w_t generated by SGD after t time steps,*

$$\frac{1}{\sqrt{t}}(\ln |w_t/w_0| - \mu) \rightarrow_d \mathcal{N}(0, s^2) \quad (26)$$

where $\mu = \mathbb{E}_x[\ln |1 - \lambda x|]$ and $s^2 = \text{Var}[\ln |1 - \lambda x|]$, where $\lambda > 0$ is the learning rate.

Proof. After t steps of SGD, we have

$$w_t = \prod_{i=1}^t [1 - \lambda x_i] w_0. \quad (27)$$

This leads to

$$\ln \left| \frac{w_t}{w_0} \right| = \sum_{i=1}^t \ln |1 - \lambda x_i|. \quad (28)$$

Now, since $p(1 - x)$ is continuous in the neighborhood of 1 by assumption, we can apply Proposition 6 (appendix) to show that the first and second moment of $\ln |1 - \lambda x|$ exists, whereby we can apply the central limit theorem to obtain

$$\frac{1}{\sqrt{t}} \left(\ln \left| \frac{w_t}{w_0} \right| - t \mathbb{E}[\ln |1 - \lambda x|] \right) \rightarrow_d \mathcal{N}(0, s^2), \quad (29)$$

where $s^2 = \text{Var}[\ln |1 - \lambda x|]$. This proves the lemma. \square

Proposition 6. $\mathbb{E}_{x \sim p(x)}[\ln^2 |x|]$ is finite if the second moment of $p(x)$ exists and if $p(x)$ is continuous in the neighborhood of $x = 0$.

Proof. Since $p(x)$ is continuous in the neighborhood of $x = 0$, then there exists $\delta > 0$ such that for all $|\epsilon| < \delta$, $|p(\delta) - p(x)| \leq c$ for some $c > 0$. This means that we can divide the integral over $p(x)$ into three regions:

$$\mathbb{E}_{x \sim p(x)}[\ln^2 |x|] = \int_{-\infty}^{\infty} dx p(x) \ln^2 |x| \quad (30)$$

$$= \int_{-\infty}^{-\delta} dx p(x) \ln^2 |x| + \int_{-\delta}^{\delta} dx p(x) \ln^2 |x| + \int_{\delta}^{\infty} dx p(x) \ln^2 |x|. \quad (31)$$

The second term can be bounded as

$$\int_{-\delta}^{\delta} dx p(x) \ln^2 |x| \leq [p(0) + c] \int_{-\delta}^{\delta} dx \ln^2 |x| \quad (32)$$

$$= 2[p(0) + c] \int_0^{\delta} dx \ln^2 x \quad (33)$$

$$= 2[p(0) + c] x (\ln^2 x - 2 \ln x + 2) \Big|_0^{\delta} \quad (34)$$

$$= 2[p(0) + c] \delta (\ln^2 \delta - 2 \ln \delta + 2) < \infty. \quad (35)$$

The first and the third term can also be bounded. Since $\ln |x|$ is a convex function in the regions $x \gg \delta$ and $x \leq \delta$ respectively. We can find linear functions $ax + b$ of x such that $ax + b \geq \ln x$ for $x \gg \delta$. This leads

to

$$\int_{\delta}^{\infty} dx p(x) \ln^2 |x| \leq \int_{\delta}^{\infty} dx p(x) (ax + b)^2 \quad (36)$$

$$\leq \int_{-\infty}^{\infty} dx p(x) (ax + b)^2 \quad (37)$$

$$= \int_{-\infty}^{\infty} dx p(x) (a^2 x^2 + 2abx + b^2) \quad (38)$$

$$= a^2 \mu_2 + 2ab\mu_1 + b^2, \quad (39)$$

where we have used the notation $\mathbb{E}[x^2] = \mu_2$ and $\mathbb{E}[x] = \mu$, which by assumption is finite. The case for $x \leq -\delta$ is completely symmetric and can also be bounded by $a^2 \mu_2 + 2ab\mu_1 + b^2$. Therefore, we have shown that

$$\mathbb{E}_{x \sim p(x)}[\ln |x|^2] \leq 2(a^2 \mu_2 + 2ab\mu_1 + b^2) + 2(p(0) + c)\delta(\ln^2 \delta - 2 \ln \delta + 2) \leq \infty. \quad (40)$$

This proves the proposition. \square

Remark. Note that, the continuity in the neighborhood of 0 is not an necessary condition. For example, one can also prove that $\mathbb{E}_x[\ln^2 |x|]$ is finite if $p(x)$ is bounded and its second moment exists.

B.2 Case of Gaussian Noise

In this section, we treat the case when the noise is Gaussian. As discussed in the main text, this regime can be seen as the SGD with a large batch-size.² In this case, one can still find the condition such that the SGD is attracted to the local maximum; however, this condition is no longer analytically solvable.

Proposition 7. Let $\lambda > 0$ be any fixed real value, and let the data points x obey an Gaussian distribution; there exists a loss function such that SGD converges to a local maximum with probability 1.

Proof. Still, let the loss function be

$$L(w) = \frac{x}{2} w^2, \quad (41)$$

where $x \sim \mathcal{N}(-a, \sigma^2)$ obeys an Gaussian distribution. The loss function can be equivalently written as

$$L(w) = \frac{-a}{2} w^2 + \frac{\sigma \epsilon}{2} w^2 \quad (42)$$

where $\epsilon \sim \mathcal{N}(0, 1)$. After t time-steps, we have

$$w_t = \prod_{i=1}^t [1 - \lambda(a + \sigma \epsilon_i)] w_0. \quad (43)$$

This leads to

$$\ln \left| \frac{w_t}{w_0} \right| = \sum_{i=1}^t \ln |1 - \lambda(a + \sigma \epsilon_i)|. \quad (44)$$

We now define $\mu = \mathbb{E}[\ln |1 - \lambda(a + \sigma \epsilon)|]$, and $s^2 = \text{Var}[\ln |1 - \lambda(a + \sigma \epsilon)|]$, which can be identified by finding the distribution of $\ln |1 - \lambda(a + \sigma \epsilon)|$. By the law of large numbers, we introduce the random variable z :

$$z_t := \frac{1}{\sqrt{t}} \ln \left| \frac{w_t}{w_0} \right| - \frac{1}{\sqrt{t}} \mathbb{E} \left[\ln \left| \frac{w_t}{w_0} \right| \right] = \frac{1}{\sqrt{t}} \sum_{i=1}^t (\ln |1 - \lambda(a + \sigma \epsilon_i)| - \mu) \rightarrow_d \mathcal{N}(0, s^2) \quad (45)$$

²In our experience, a batch size larger than 64 would already result in a gradient distribution quite well approximated by a Gaussian.

By definition, $|w_t| = |w_0|e^{\sqrt{t}z+t\mu}$. Performing a transformation of random variables, we obtain that

$$\begin{aligned}
P(w) &= \lim_{t \rightarrow \infty} P(w_t) = \lim_{t \rightarrow \infty} P(z_t) \left| \frac{dz}{d|w_t|} \right| + o(1) \\
&= \lim_{t \rightarrow \infty} \frac{1}{\sqrt{2\pi s^2}} \exp \left[-\frac{1}{2s^2} \left(\frac{1}{\sqrt{t}} \ln \left| \frac{w_t}{w_0} \right| - \sqrt{\mu} \right)^2 \right] \times \frac{1}{\sqrt{t}|w_t|} \\
&= \lim_{t \rightarrow \infty} \frac{1}{\sqrt{2\pi t s^2}} \frac{1}{|w_t|} \exp \left[-\frac{1}{2ts^2} \left(\ln \left| \frac{w_t}{w_0} \right| - t\mu \right)^2 \right]. \tag{46}
\end{aligned}$$

We again have the limit of a log-normal distribution with mean $\sqrt{t}\mu$ and standard deviation $\sqrt{t}s$. The p -quantile is, as before,

$$\exp \left[t\mu + \sqrt{2ts} \operatorname{erf}^{-1}(2p - 1) \right]. \tag{47}$$

In the infinite t limit, the sign of μ becomes crucial. When $\mu > 0$, the limiting distribution diverges to infinity; when $\mu < 0$, the limiting distribution is a Dirac delta distribution $\delta(w)$. \square

C Continuous-Time Approximation with Fokker-Planck Equation

C.1 Fokker-Planck Equation and Its Stationary Distribution

In this section, we approach the relevant problems in this paper using continuous-time approximation. In fact, many results we have obtained in discrete-time can also be derived in continuous-time. One advantage of the continuous-time limit is that the distribution of w now only depends on the second moment of x and no more depends on the distribution of the $p(x)$, and, therefore, the results become independent of the actual distribution of $p(x)$.

The additional advantage of continuous-time approximation is that it gives us more flexibility to deal with more complicated loss landscapes. Recall that the SGD update takes the form (see Section 2)

$$\Delta w_t = -\lambda \nabla L + \lambda \sqrt{C} \eta_t, \quad (48)$$

when $\lambda < 1$, the above equation may be approximated by a continuous-time Ornstein-Uhlenbeck process (Mandt et al., 2017)

$$dw(t) = -\lambda \nabla L dt + \frac{\lambda}{\sqrt{S}} \sqrt{C(w)} dW(t), \quad (49)$$

where λ is the learning rate; we have also introduced S as the batch size. $dW(t)$ is a stochastic process satisfying

$$\begin{cases} dW(t) \sim \mathcal{N}(0, dtI), \\ \mathbb{E}[dW(t)dW(t')] \propto \delta(t-t'). \end{cases} \quad (50)$$

By the definition of the underlying discrete-time process, the term $dw(t)$ depends only on $w(t)$ and has no dependence on $w(t+dt)$. Thus, the stochastic integration should be interpreted as Ito, and this leads to the following Fokker-Planck equation (Risken, 1996).

$$\frac{\partial P[w, t|w(0), 0]}{\partial t} = \lambda \nabla \cdot \{(\nabla L)P[w, t|w(0), 0]\} + \frac{\lambda^2}{2S} \text{Tr}(\nabla \nabla^T \{C(w)P[w, t|w(0), 0]\}), \quad (51)$$

where $\text{Tr}[\cdot]$ is the trace.

For simplicity, only one dimensional version of the Fokker-Planck equation is considered, which is

$$\frac{\partial P[w, t|w(0), 0]}{\partial t} = \lambda \frac{\partial}{\partial w} \left\{ \frac{\partial L}{\partial w} P[w, t|w(0), 0] \right\} + \frac{\lambda^2}{2S} \frac{\partial^2}{\partial w^2} \{C(w)P[w, t|w(0), 0]\}. \quad (52)$$

The probability $P[w, t|w(0), 0]$ is normalized by definition, thus, the total probability is conserved. Expressing this relation in a microscopic manner, one finds

$$\frac{\partial P[w, t|w(0), 0]}{\partial t} = -\frac{\partial}{\partial w} J(w, t|w(0), 0), \quad (53)$$

where $J[w, t|w(0), 0]$ is the probability flow. Comparing with the Fokker-Planck equation, the expression of $J[w, t|w(0), 0]$ is obtained:

$$J[w, t|w(0), 0] = \lambda \frac{\partial L}{\partial w} P[w, t|w(0), 0] + \frac{\lambda^2}{2S} \frac{\partial}{\partial w} \{C(w)P[w, t|w(0), 0]\}. \quad (54)$$

Assuming that the SGD dynamics is ergodic, there is a single stationary distribution for w when $t \rightarrow \infty$, and it satisfies

$$0 = \lambda \frac{\partial}{\partial w} \left[\frac{\partial L}{\partial w} P(w) \right] + \frac{\lambda^2}{2S} \frac{\partial^2}{\partial w^2} [C(w)P(w)]. \quad (55)$$

The dependence on the initial condition could be dropped due to ergodicity. Integrating over w on both sides, one finds

$$J_0 = \lambda \frac{\partial L}{\partial w} P(w) + \frac{\lambda^2}{2S} \frac{\partial}{\partial w} [C(w)P(w)]. \quad (56)$$

where J_0 is the integral constant, which could be interpreted as the stationary flow of probability going from $-\infty$ to ∞ . When the loss function is convex, $P(\infty) = 0$. Thus this flow is naturally 0. In this case, the stationary solution takes a simple form:

$$P(w) \propto \frac{1}{C(w)} \exp\left[-\frac{2S}{\lambda} \int dw \frac{1}{C(w)} \frac{\partial L}{\partial w}\right]. \quad (57)$$

We will apply this equation to the study of the relevant problems in this work.

C.2 Additive plus Multiplicative Noise

In this section, we consider (a slightly more general version of) the fourth-order potential we studied in the main text. The loss landscape in this model is

$$L(w) = \frac{1}{2}aw^2 + \frac{1}{4}bw^4. \quad (58)$$

We set $b > 0$ guarantees that the w is bounded regardless the value of a . In the limit of $b \rightarrow 0$, this function reduces to saddle point problem we studied in Section 5.1. Besides the SGD noise, additive noise is also present in the dynamics. Unlike the SGD noise, the variance of the additive noise has no dependence on w . When the additive noise is present, the update rule (equation of motion) becomes

$$dw(t) = -[\lambda aw(t) + bw^3(t)]dt + \lambda\eta_m(t) + \lambda\eta_a(t), \quad (59)$$

where both $\eta_m(t)$ and $\eta_a(t)$ are both Ornstein-Uhlenbeck process. The w -dependent covariance of w is $C(w) = w^2$. The SGD noise is thus a multiplicative noise $\eta_m(t)$ and has a variance $\frac{w(t)^2}{S}dt$, while the additive noise $\eta_a(t)$ has a variance of σ^2dt . There is no correlation between the additive noise and the SGD noise, i.e. $\mathbb{E}[\eta_m(t)\eta_a(t')] = 0$. σ is a positive constant denoting the strength of the additive noise. The additive noise can be seen as the artificially injected noise, a technique sometimes used for helping with the escape or for Bayesian learning purposes (Jin et al., 2017; Welling and Teh, 2011).

The additive noise vanishes in the limit of $\sigma \rightarrow 0$, and the model becomes a normal SGD with 4th-order loss function. It is always possible to define a noise $\eta'(t)$, whose contribution is equivalent to the contribution of both the SGD and the additive noise, and the equation of motion becomes

$$dw(t) = -[\lambda aw(t) + bw^3(t)]dt + \lambda\eta'(t). \quad (60)$$

This transformed noise $\eta'(t)$ thus has 0 mean and a variance of $\left(\frac{w(t)^2}{S} + \sigma^2\right)dt$. Define $\eta(t) = \eta'(t)/\sqrt{\frac{w(t)^2}{S} + \sigma^2}$, the equation of motion becomes

$$dw(t) = -\lambda[aw(t) + bw^3(t)]dt + \lambda\sqrt{\frac{w(t)^2}{S} + \sigma^2}\eta(t). \quad (61)$$

Comparing with (49), one finds

$$C(w) = w^2 + S\sigma^2 \quad (62)$$

The solution of the corresponding Fokker-Planck equation is

$$\begin{aligned} P(w) &\propto \frac{1}{w^2 + S\sigma^2} \exp\left[-\frac{2S}{\lambda} \int \frac{aw + bw^3}{w^2 + S\sigma^2} dw\right] \\ &= (w^2 + S\sigma^2)^{-1} \exp\left[-\frac{2Sb}{\lambda} \int \frac{\left(\frac{a}{b} - S\sigma^2\right)w + w^3 + S\sigma^2w}{w^2 + S\sigma^2} dw\right] \\ &= (w^2 + S\sigma^2)^{-1} \exp\left[-\frac{2Sb}{\lambda} \int w dw - \frac{2Sb}{\lambda} \left(\frac{a}{b} - S\sigma^2\right) \int \frac{w}{w^2 + S\sigma^2} dw\right] \\ &= (w^2 + S\sigma^2)^{-1} \exp\left[-\frac{Sb}{\lambda} w^2 - \left(\frac{Sa}{\lambda} - \frac{S^2\sigma^2b}{\lambda}\right) \ln(w^2 + S\sigma^2)\right] \end{aligned}$$

Simplifying, one finds

$$P(w) \propto (w^2 + S\sigma^2)^{-1 - \frac{Sa}{\lambda} + \frac{S^2b\sigma^2}{\lambda}} \exp\left[-\frac{Sb}{\lambda}w^2\right]. \quad (63)$$

The function $P(w)$ is finite everywhere and decays to 0 exponentially fast when $w \rightarrow \infty$. This indicates that $\int_{-\infty}^{\infty} dw (w^2 + S\sigma^2)^{-1 - \frac{Sa}{\lambda} + \frac{S^2b\sigma^2}{\lambda}} \exp\left[-\frac{Sb}{\lambda}w^2\right]$ has a well-defined value. The other thing one can learn from $P(w)$ is that there is no concentration of measure. Since the measure is not concentrated at a point, $w(t)$ can be fall into any interval with finite probability. Thus, with a t that is big enough, $w(t)$ can be arbitrarily far away from 0. In practice, this means $w(t)$ escaping from the saddle point at $w = 0$.

In the language of Bayesian inference, $\ln[P(w)]$ is the likelihood of w . \hat{w} , the most probable value of w , is defined by the relation

$$\left. \frac{d \ln [P(w)]}{dw} \right|_{w=\hat{w}} = 0. \quad (64)$$

which reads

$$\begin{aligned} 0 &= \frac{d}{dw} \left[\left(-1 - \frac{Sa}{\lambda} + \frac{S^2b\sigma^2}{\lambda} \right) \ln [(w^2 + S\sigma^2)] - \frac{Sb}{\lambda} w^2 \right] \\ &= 2w \frac{-1 - \frac{Sa}{\lambda} + \frac{S^2b\sigma^2}{\lambda}}{w^2 + S\sigma^2} - \frac{2Sb}{\lambda} w \\ &= w \left[-1 - \frac{Sa}{\lambda} + \frac{S^2b\sigma^2}{\lambda} - \frac{Sb}{\lambda} (w^2 + S\sigma^2) \right] \\ &= w \left(\frac{\lambda}{Sb} + \frac{a}{b} + w^2 \right) \end{aligned}$$

The likelihood maximizer is

$$\hat{w} = \begin{cases} 0, & a > -\frac{\lambda}{S}; \\ \pm \sqrt{-\frac{\lambda}{Sb} - \frac{a}{b}}, & a < -\frac{\lambda}{S}. \end{cases} \quad (65)$$

When $a > -\frac{\lambda}{S}$, the maximum likelihood parameter is $w = 0$. When $a < -\frac{\lambda}{S}$, $w = \pm \sqrt{-\frac{\lambda}{Sb} - \frac{a}{b}}$ are equally likely. From the energy landscape, when $a > 0$, there is only one global minimum at $w = 0$, and when $a < 0$, there are two global minima at $w = \pm \sqrt{-\frac{a}{b}}$. Comparing with the maximum likelihood solutions, we see that the SGD is in fact a biased estimator of the underlying minima.

There is a bias term introduced by the SGD noise in both the critical a and the value of the most probable w . This term vanishes when $S \rightarrow \infty$, i.e. when the SGD noise vanishes. This indicates that, when the noise is state-dependent, there is no reason to expect SGD to be an unbiased or consistent estimator of the minimizer, as some works assume.

C.3 4-th Order Potential with Multiplicative Noise

In this subsection, we study a 4-th order loss landscape in SGD dynamics without additive noise. The 1d loss function with 4-th order term is

$$L(w) = \frac{aw^2}{2} + \frac{xw^2}{2} + \frac{bw^2}{4}; \quad (66)$$

the SGD update rule (i.e., the equation of motion) in this case is

$$dw(t) = -\lambda[aw(t) + bw^3(t)]dt + \lambda \frac{1}{\sqrt{S}} \eta(t)w(t), \quad (67)$$

where the definition of η is identical to the previous example. The solution of corresponding stationary Fokker-Planck equation is

$$P(w) \propto w^{-2 - \frac{2Sa}{\lambda}} \exp\left[-\frac{Sb}{\lambda}w^2\right]. \quad (68)$$

When

$$-\frac{Sa}{\lambda} < 1, \quad (69)$$

$P(w)$ diverges at $w = 0$. The normalization factor, i.e. integral $\int_{-\infty}^{+\infty} dw w^{-2-\frac{2Sa}{\lambda}} \exp\left[-\frac{Sb}{\lambda} w^2\right]$, also diverges due to the divergence at $w = 0$. This solution could be seen as a limit of (63) when the additive noise vanishes. As the strength of the additive noise $\sigma \rightarrow 0$, the normalization factor keep growing and the distribution remains normalized. For $w \neq 0$, the function $w^{-2-\frac{2Sa}{\lambda}} \exp\left[-\frac{Sb}{\lambda} w^2\right]$ is always finite. Thus, in the limit $\sigma \rightarrow 0$, $P(w)$ is 0 everywhere except for 0. It is straight forward to check that the normalization factor diverges slower than $P(0)$ as $\sigma \rightarrow 0$. As a consequence, when $\sigma = 0$, $P(w)$ diverges at $w = 0$. Thus, $P(w)$ becomes a Dirac delta function. This corroborates with the result in Section 5.3 that a small a leads to a concentration of measure towards the local maximum.

Compared with (63), one finds that the additive noise prevents the concentration of measure. Thus, in practice, the additive noise helps SGD escape the local minimum or saddle point. However, whether there is additive noise or not does not change the critical value of a and the position of the peaks.

C.4 Quadratic Potential

At last, we consider the continuous approximation of the model treated in the Section 5.1. Let the loss function be

$$\hat{L} = \frac{x}{2} w^2, \quad (70)$$

and we have

$$\begin{cases} \mathbb{E}_x[\hat{g}_t] = aw_t \\ C(w_t) = \frac{1}{S} \mathbb{E}[\nabla \ell \nabla \ell^T] - \frac{1}{S} \nabla; L(\mathbf{w}_t) \nabla L(\mathbf{w}_t)^T = \frac{1}{S} (\mathbb{E}[x^2] w_t^2 + a^2 w_t^2). \end{cases} \quad (71)$$

The SGD update rule (i.e., the equation of motion) is

$$\Delta w(t) = -\lambda \frac{\partial}{\partial w} \hat{L}; \quad (72)$$

$$= -\lambda aw(t) - \lambda xw(t). \quad (73)$$

With the continuous approximation, the equation of motion becomes

$$dw(t) = -\lambda aw(t) dt + \lambda \frac{1}{\sqrt{S}} \eta(t) w(t), \quad (74)$$

where $\eta(t) \sim \mathcal{N}(0, \sqrt{dt})$. By comparing with the 1d Fokker-Planck equation,

$$\begin{cases} L(w) = \frac{a}{2} w^2; \\ B(w) = w. \end{cases} \quad (75)$$

The stationary distribution of w is

$$P(w) \propto \frac{1}{w^2} \exp\left[-\frac{2S}{\lambda} \int dw \frac{a}{w}\right] \propto w^{-2-\frac{2Sa}{\lambda}}; \quad (76)$$

$w^{-2-\frac{2Sa}{\lambda}}$ diverges when $w = 0$ or $w = \pm\infty$. However, the stationary distribution in this model could be defined as a limit of (63). When it diverges at $w = 0$, $P(w)$ becomes a delta function. On the contrary, there are two peaks far away from 0 when $w^{-2-\frac{2Sa}{\lambda}}$ diverges at $w = \pm\infty$. Compared with the 4-th order loss case, the 4th-order potential introduces an exponential factor, showing that the only function of the 4th-order potential is to keep $w(t)$ bounded. Being able to escape $w = 0$ requires

$$-\frac{Sa}{\lambda} > 1. \quad (77)$$

Note that this line agrees with the boundary of the lower branch of the phase diagram in Figure 3 when $a \rightarrow 0$. Also, note that, in the continuous-time approximation, the result only depends on the second moment

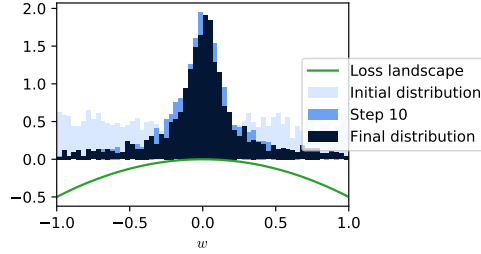


Figure 9: Stationary distribution of w with additive noise of $\sigma = 0.1$ with quadratic loss landscape. All the other parameters are identical to Fig.1. Though the stationary distribution exists, it is not a delta function.

of x and is independent of its distribution. This suggests that the results discovered in this work may apply to much more general situations than we have assumed in the main text.

Fig.9 shows the stationary distribution of w when there is additive noise. The other settings are identical to the ones in Fig.1. The stationary distribution exists, but w are not concentrated at $w = 0$ in the stationary distribution. First of all, this figure shows that the additive noise aides SGD to escape saddle point. If the designed landscape is a part of a realistic landscape, having a broader distribution means having more chance of being attracted by another minimum. However, this figure also shows that w would stay in the neighbourhood of $w = 0$ until the noise is big enough. Thus, having additive noise and long enough training time does not guarantee the efficiency of escape.

D Delayed Proofs

D.1 Proof of Proposition 2

Proof. By Lemma 1 (alternatively, we can apply the De Moivre-Laplace theorem), we have

$$\frac{1}{\sqrt{t}}z_t \rightarrow_d \mathcal{N}(0, s^2) \quad (78)$$

where we have defined $z_t = \frac{1}{\sqrt{t}}(\ln \left| \frac{w_t}{w_0} \right| - t\mu)$, $\mu = \mathbb{E}[\ln |1 - \lambda x|]$ and $s^2 = \text{Var}[\ln |1 - \lambda x|]$. This means that

$$\lim_{t \rightarrow \infty} p \left(\frac{1}{\sqrt{t}} \ln \left| \frac{w_t}{w_0} \right| \right) = \lim_{t \rightarrow \infty} \frac{1}{\sqrt{2\pi s^2}} \exp \left[-\frac{1}{2ts^2} \left(\ln \left| \frac{w_t}{w_0} \right| - t\mu \right)^2 \right]. \quad (79)$$

By definition, $|w_t| = |w_0|e^{\sqrt{t}z + t\mu}$. Therefore, we have

$$\lim_{t \rightarrow \infty} P(|w_t| > \epsilon) = \lim_{t \rightarrow \infty} P(|w_0|e^{\sqrt{t}z + t\mu} > \epsilon) = \begin{cases} 0 & \text{if } \mu < 0 \\ 1 & \text{if } \mu > 0, \end{cases} \quad (80)$$

for all $\epsilon > 0$. In other words, since μ and σ are t -independent, in the infinite t limit, the sign of μ becomes crucial. When $\mu > 0$, the limiting distribution diverges to infinity; when $\mu < 0$, $|w_t|$ converges to 0 in probability.

By the definition of $p(x)$,

$$\mu = \mathbb{E}[\ln |1 - \lambda x|] \quad (81)$$

$$= \frac{1}{2} \ln |1 - \lambda| + \frac{1}{2} \ln |1 - \lambda(a - 1)| \quad (82)$$

$$= \frac{1}{2} \ln |(1 - \lambda)(1 - \lambda(a - 1))|, \quad (83)$$

while s^2 is indeed constant in time. Therefore, the asymptotic distribution of w_t is solely dependent on the sign of μ . The above equation implies that $\mu \geq 0$ when

$$|(1 - \lambda)[1 - \lambda(a - 1)]| > 1 \quad (84)$$

When $\lambda \leq 1$, the above equation is solved by

$$\lambda < \frac{a}{a - 1}. \quad (85)$$

When $\lambda > 1$, the above equation solves to

$$\lambda \geq \frac{a - \sqrt{a^2 - 8a + 8}}{2(a - 1)}, \quad (86)$$

only when the learning rate satisfies the above two conditions can it escape from the local maximum. Conversely, SGD cannot escape the local minimum when

$$\frac{a}{a - 1} \leq \lambda \leq \frac{a - \sqrt{a^2 - 8a + 8}}{2(a - 1)} \quad (87)$$

This proves the proposition. \square

D.2 Proof of Proposition 3

Proof. By Lemma 1, we have that

$$\frac{1}{t} \mathbb{E} \left[\ln \left| \frac{w_t}{w_0} \right| \right] = \mu = \frac{1}{2} \ln \{(1 - \lambda)[1 - \lambda(a - 1)]\}, \quad (88)$$

where the second equality follows from the assumption that $\lambda < 1$. We differentiate with respect to λ to find the critical escape rate:

$$\lambda^* = \frac{a}{2(a-1)}. \quad (89)$$

Since μ is convex in λ , it follows that this critical escape rate is the maximum escape rate. Plug this into μ , we obtain that

$$\gamma^* = \mu(\lambda^*) = \frac{1}{2} \ln \frac{(2-a)^2}{4(1-a)} = \ln \frac{2-a}{2\sqrt{1-a}} \leq \epsilon, \quad (90)$$

i.e., the optimal escape rate can be made smaller than any ϵ if we set

$$|a| \leq 2 \left| -e^\epsilon \sqrt{e^{2\epsilon} - 1} - e^{2\epsilon} + 1 \right|. \quad (91)$$

This finishes the proof. \square

D.3 Proof of Proposition 4

Proof. It suffices to show that w_1 converges to 0 with probability 1 because, if this is the case, the only possible local minimum to converge to is $(w_1, w_2) = (0, \pm\sqrt{\frac{1+a}{2}})$.

The SGD dynamics is

$$\begin{cases} \Delta w_{1,t} = -\lambda(-2w_{1,t} + 4w_{1,t}^3 + 12w_{2,t}^2 w_{1,t} + x_t b w_{1,t}) \\ \Delta w_{2,t} = -\lambda(-2w_{2,t} + 4w_{2,t}^3 + 12w_{1,t}^2 w_{2,t} - 2a w_{2,t}). \end{cases} \quad (92)$$

We focus on the dynamics of w_1 . By the definition of the noise x , we have that

$$w_{1,t+1} = \begin{cases} w_{1,t}[1 + \lambda(2-b) - 4\lambda w_{1,t}^2 - 12\lambda w_{2,t}^2] & \text{with probability } 1/2; \\ w_{1,t}[1 + \lambda(2+b) - 4\lambda w_{1,t}^2 - 12\lambda w_{2,t}^2] & \text{with probability } 1/2. \end{cases} \quad (93)$$

Equivalently,

$$\left| \frac{w_{1,t+1}}{w_{1,t}} \right| = \begin{cases} |1 + \lambda(2-b) - 4\lambda w_{1,t}^2 - 12\lambda w_{2,t}^2| & \text{with probability } 1/2; \\ |1 + \lambda(2+b) - 4\lambda w_{1,t}^2 - 12\lambda w_{2,t}^2| & \text{with probability } 1/2. \end{cases} \quad (94)$$

Since $0 \leq 4\lambda w_{1,t}^2 + 12\lambda w_{2,t}^2 \leq 16\lambda$, we can define a new random variable r_t :

$$r_t := r(x_t) := \begin{cases} \max(|1 + \lambda(2-b)|, |1 + \lambda(2-b) - 16\lambda|) & \text{if } x_t \geq 0; \\ \max(|1 + \lambda(2+b)|, |1 + \lambda(2+b) - 16\lambda|) & \text{if } x_t \leq 0. \end{cases} \quad (95)$$

By construction, $r_t \geq |w_{1,t+1}/w_{1,t}|$ for all values of x_t . This implies that $|w_{1,t}/w_{1,0}| \leq \prod_{i=1}^t r_i$, and so,

$$P(|w_{1,t}/w_{1,0}| > \epsilon) \leq P\left(\prod_{i=1}^t r_i > \epsilon\right), \quad (96)$$

i.e., if $\prod_{i=1}^t r_i$ converges to 0 with probability 1, $w_{1,t}$ must also converge to zero with probability 1.

We let $b = \frac{1}{\lambda} - 6$ (note that this is the value of b such that r_t is minimized for both cases), and we obtain that

$$r_t = \begin{cases} 8\lambda & \text{if } x_t \geq 0; \\ 2 \max(|1 - 2\lambda|, |1 - 10\lambda|) & \text{if } x_t \leq 0. \end{cases} \quad (97)$$

The rest of the proof follows from applying the central limit theorem to $\frac{1}{\sqrt{t}} \sum_{i=1}^t \ln r_i$ as in Lemma 1. The result is that $\prod_{i=1}^t r_i$ converges to 0 with probability 1 if

$$\mu := \mathbb{E}[\ln r_t] = \frac{1}{2} \ln[8\lambda \max(|1 - 2\lambda|, |1 - 10\lambda|)] < 0. \quad (98)$$

The above inequality solves to

$$\lambda \leq \frac{1}{20}(1 + \sqrt{6}) \quad (99)$$

which is of order $O(1)$ as stated in the theorem statement. This proves the proposition. \square

D.4 Proof of Proposition 5

Proof. First we note that, since $|w_t| \leq 1$

$$|\hat{g}_t| = |x_t w_t| \leq 1 + a. \quad (100)$$

By the definition of the AMSGrad algorithm, we have that

$$v_t = \beta_2 v_{t-1} + (1 - \beta_2) \hat{g}_t^2; \quad (101)$$

$$\hat{v}_t = \max(\hat{v}_{t-1}, v_t). \quad (102)$$

Since $v_0 = 0$ and $|\hat{g}_t| = |x_t w_t| \leq 1 + a$, we have that

$$v_t \leq 1 + a \quad (103)$$

for all t , and so

$$\hat{v}_t \leq \max_t \hat{v}_t = \max_t v_t \leq 1 + a. \quad (104)$$

Meanwhile, since \hat{v}_t is a monotonically increasing series and is upper bounded by $1 + a$, it must converge to a constant $0 < c \leq 1 + a$.

Now, as before, we want to upper bound the random variable

$$\frac{1}{\sqrt{t}} \left(\ln \left| \frac{w_{t+1}}{w_t} \right| - \mu \right) = \frac{1}{\sqrt{t}} \sum_{i=1}^t \left(\ln \left| 1 - \frac{\lambda}{\sqrt{\hat{v}_i}} x_i \right| - \mu \right) \quad (105)$$

where $\mu = \mathbb{E}[\ln \left| \frac{w_{t+1}}{w_t} \right|]$. Since \hat{v}_t converges to c , there must exist a positive integer $N(\epsilon)$ such that for any $\epsilon > 0$, $\hat{v}_N \leq c - \epsilon$. This allows us to divide the sum to two terms:

$$\frac{1}{\sqrt{t}} \left(\ln \left| \frac{w_{t+1}}{w_t} \right| - \mu \right) = \frac{1}{\sqrt{t}} \sum_{i=1}^t \left(\ln \left| 1 - \frac{\lambda}{\sqrt{\hat{v}_i}} x_i \right| - \mu \right) \quad (106)$$

$$= \frac{1}{\sqrt{t}} \sum_{i=1}^N \left(\ln \left| 1 - \frac{\lambda}{\sqrt{\hat{v}_i}} x_i \right| - \mu \right) + \frac{1}{\sqrt{t}} \sum_{i=N+1}^t \left(\ln \left| 1 - \frac{\lambda}{\sqrt{c - k_t}} x_i \right| - \mu \right) \quad (107)$$

where we introduced $0 \leq k_t \leq \epsilon$. But the first term is of order $O(1/\sqrt{t})$ and converges to 0, and so for sufficiently large t , the first term is also smaller than arbitrary ϵ . This means that

$$\frac{1}{\sqrt{t}} \left(\ln \left| \frac{w_{t+1}}{w_t} \right| - \mu \right) \leq \frac{1}{\sqrt{t}} \sum_{i=1}^t \left(\ln \left| 1 - \frac{\lambda}{\sqrt{c - k_t}} x_i \right| - \mu \right) + \epsilon \quad (108)$$

We can now consider the random variable

$$\left| 1 - \frac{\lambda}{\sqrt{c - k_t}} x_t \right| = \begin{cases} \left| 1 - \frac{\lambda}{\sqrt{\hat{v}_t}} \right| & \text{with probability } \frac{1}{2}; \\ 1 + \frac{\lambda}{\sqrt{\hat{v}_t}} (1 - a) & \text{with probability } \frac{1}{2}. \end{cases} \quad (109)$$

We now define a new random variable

$$r_t(x_t) := \begin{cases} m & \text{if } x_t = 1; \\ 1 + \frac{\lambda}{\sqrt{c - \epsilon}} (1 - a) & \text{if } x_t = -1 + a. \end{cases} \quad (110)$$

where we defined the constant $m := \max(|1 - \lambda/\sqrt{c}|, |1 - \lambda/\sqrt{c - \epsilon}|)$. One can easily check that $r_t \geq \left| 1 - \frac{\lambda}{\sqrt{c - k_t}} x_t \right|$. This means that

$$P \left(\left| \frac{w_{t+1}}{w_0} \right| > \alpha \right) \leq P \left(\prod_{i=0}^t r_i > \alpha + O(1/\sqrt{t}) \right), \quad (111)$$

i.e., if r_t converges to 0 in probability, $\left| \frac{w_{t+1}}{w_0} \right|$ must also converge to 0 in probability. Proceeding as in the proof of Proposition 2. One finds that the condition for r_t to converge in probability to 0 is

$$\ln \left| m \left[1 + \frac{\lambda}{\sqrt{c - \epsilon}} (1 - a) \right] \right| < 0, \quad (112)$$

which is equivalent to

$$\left| m \left[1 + \frac{\lambda}{\sqrt{c}}(1-a) \right] \right| < 1. \quad (113)$$

Since ϵ is arbitrary, we let $\epsilon \rightarrow 0$ and obtain

$$\left| \left(1 - \frac{\lambda}{\sqrt{c}} \right) \left[1 + \frac{\lambda}{\sqrt{c}}(1-a) \right] \right| \leq 1. \quad (114)$$

Denote λ/\sqrt{c} as λ' , this condition solves to

$$\frac{a}{a-1} \leq \lambda' \leq \frac{a - \sqrt{a^2 - 8a + 8}}{2(a-1)}. \quad (115)$$

Setting a such that the above condition is met, AMSGrad will converge to 0 in probability. For $\lambda < 1$, This completes the proof. \square

D.5 A Conjecture about the Importance of the Noise

The mathematical constructions in this work may all be related to the following conjecture: *if the noise is arbitrary, SGD may converge to any stationary distribution.* Surprisingly, we can prove this hypothesis in one dimension and when continuous-approximation is adopted. In continuous-time, SGD is equivalent to the following stochastic differential equation (SDE):

$$\dot{w} = -\nabla_w L(w) + C(w)\eta(t) \quad (116)$$

where $\eta(t)$ is a zero-mean noise with unit variance, and $C(w)$ is the w -dependent variance of the noise.

Proposition 8. *Let $w \in \mathbb{R}$, the loss function $L(w)$ be an arbitrary differential function, and $p(w)$ be an any distribution such that $0 < p(w) < \infty$ and $\lim_{w \rightarrow \infty} wL'(w)p(w) < \infty$. Then there exists $C(w)$ such that the stationary distribution of SGD is $p(w)$*

We prove this proposition below. This proposition shows that if the noise is arbitrary (even if it is smooth and zero-mean), the stationary distribution of SGD can be independent of the landscape as long as it is sufficiently regular and smooth. It is possible to extend this proposition to some (mildly) non-smooth distributions. This result becomes more surprising since we can show that the converse is not true, i.e., for an arbitrary $p(w)$, there exists $C(w)$ such that there is no $L(w)$ such that $p_S(w) = p(w)$.

Proposition 9. *Let $w \in \mathbb{R}$, $p(w)$ be an arbitrary (sufficiently smooth) distribution. Then there exist $C(w)$ such that the stationary distribution $p_S(w) \neq p(w)$ for any loss landscape $L(w)$.*

Proof. Simply let $C(w) = 0$, and let $p(w)$ be a Gaussian distribution with non-zero variance. Then the SDE either converges to distributions with Dirac measures or does not converge at all for any $L(w)$. \square

The above two propositions combined have an important implication: the noise may be more crucial than the landscape itself in influencing the dynamics and the convergence of SGD. This relates to the central message of this work. To study the role of SGD in deep learning, one has to make realistic assumptions about its noise, and the structure of the noise needs to be a function of the model architecture and the actual data distribution.

Before the proof of the first proposition, we state a more “constructive” version of the proposition. The proof follows by solving the Fokker-Planck equation, whose validity has been rigorously studied (Ndao, 2016). The Fokker-Planck equation and some relevant studies has been presented in Section C.

Proposition 10. *Let $w \in \mathbb{R}$, the loss function $L(w)$ be an arbitrary differential function, and $p(w)$ be an any distribution such that $0 < p(w) < \infty$ and $\lim_{w \rightarrow \infty} wL'(w)p(w) < \infty$. Then, if*

$$C(w) = \frac{1}{p(w)} \left[c_0 - \frac{2S}{\lambda} \int p(w)dL(w) \right], \quad (117)$$

the stationary distribution of SGD is $p(w)$.

Proof. The stationary distribution $p_S(w)$ is given by the solution to the Fokker-Planck equation in (56). Integrating over w , one finds

$$c_0 + J_0 w - \lambda \int p_S(w) dL(w) = \frac{\lambda^2}{2S} [C(w)p_S(w)], \quad (118)$$

where c_0 is the integration constant. For the notion-wise simplicity, c_0 multiplied or added by a constant is also denoted as c_0 . By the definition of a distribution on \mathbb{R} , $\lim_{|w| \rightarrow \infty} p_S(w) = 0$. The constant probability flow J_0 going through the system is also 0. Applying $J_0 = 0$ and rearranging the equation, one finds

$$C(w) = \frac{1}{p_S(w)} \left[c_0 - \frac{2S}{\lambda} \int p_S(w) dL(w) \right]. \quad (119)$$

The statement of this proposition is therefore equivalent to the statement that we can find $C(w) \geq 0$ such that Eq. (119) is satisfied. By assumption, $p_S(w) > 0$ everywhere; thus, the solution $C(w)$ exists if

$$c_0 - \int p_S(w) dL(w) > 0; \quad (120)$$

or, equivalently,

$$\int L'(w) p_S(w) dw := \mathbb{E}_{p_S(w)} [L'(w)] < c_0, \quad (121)$$

i.e. the average value of $L'(w)$ is upper bounded by c_0 . This condition is satisfied, when $p_S(w)$ itself is finite everywhere, by tuning $p_S(w)$ such that $\lim_{w \rightarrow \infty} wL'(w)p_S(w) < \infty$. Thus, the stationary distribution of w under SGD dynamics could be any distribution, as long as the probability distribution $p_S(w)$ satisfies

- $p_S(w) > 0$
- $p_S(w) < \infty$
- $\lim_{w \rightarrow \infty} wL'(w)p_S(w) < \infty$

This completes the proof. \square

Remark. The condition $\lim_{w \rightarrow \infty} wL'(w)p(w) < \infty$ is equivalent to saying that tail of $p(w)$ has to decay sufficiently fast. Since the loss landscape is usually polynomial, the aforementioned condition is usually satisfied in practice. Depending on $L(w)$, the condition $0 < p(w) < \infty$ could be relaxed such that $0 < p(w) < \infty$ almost everywhere.

We also would like to comment that, even if the target distribution is not smooth and does not satisfy the condition in Proposition 10, it is still possible that we can approximate $p(x)$ arbitrarily close. For example, if the target $p(x)$ is the (not necessarily smooth) limiting distribution of a sequence of smooth distributions in distance function $f([p])$, then we can still approximate $p(x)$ arbitrarily well in the specified distance function f . This allows us to extend the applicability of the above proposition to common non-smooth ones such as a delta distribution (see the example below) or a uniform distribution.

The following examples follow from direct applications of Proposition 8.

Example 1. If $L(w) = \frac{1}{2}aw^2$ and $C(w) = C(w) = w^2$, then, by Proposition 10 $p_S(w) = p(w) \propto w^{-2-\frac{2S\alpha}{\lambda}}$. When $p_S(w) = p(w) \propto w^{-2-\frac{2S\alpha}{\lambda}}$ and $L(w) = \frac{1}{2}aw^2$, according to (119),

$$\begin{aligned} C(w) &= w^{2+\frac{2S\alpha}{\lambda}} \left[c_0 - \frac{2S}{\lambda} \int w^{-2-\frac{2S\alpha}{\lambda}} d\left(\frac{1}{2}aw^2\right) \right] \\ &= w^{2+\frac{2S\alpha}{\lambda}} \left[c_0 - \frac{2Sa}{\lambda} \int w^{-1-\frac{2S\alpha}{\lambda}} dw \right] \\ &= w^{2+\frac{2S\alpha}{\lambda}} \left[c_0 + w^{-\frac{2S\alpha}{\lambda}} \right] \\ &= c_0 w^{2+\frac{2S\alpha}{\lambda}} + w^2 \end{aligned}$$

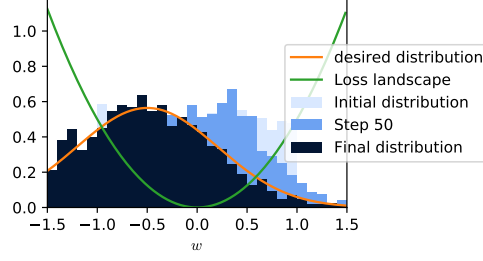


Figure 10: Distribution of the parameter w , initialized uniformly in the interval $[-1, 1]$. w is truncated at -4 and 4 . The experiment simulates a continuous-time process. With $C(w)$ and $L(w)$ from Example 2, $p(w)$ does converge to the desired distribution $p(w) = \frac{1}{\sqrt{\pi}} \exp[-(w - w_0)^2]$.

when $c_0 = 0$, $B(w) = w^2$, which is consistent with the results in the appendix. Notice that, in this example, $p_S(w)$ diverges at $w = 0$ and this distribution is defined only as a limit, where Proposition 10 still holds.

Example 2. If $L(w) = \frac{1}{2}w^2$, and $C(w) = \exp[(w - w_0)^2] \left\{ c_0 - \frac{2S}{\lambda} \int w' \exp[-(w' - w_0)^2] dw' \right\}$, then $p(w) = \frac{1}{\sqrt{\pi}} \exp[-(w - w_0)^2]$. It is straightforward to check that the expression of $C(w)$ is derived using (119). One can also check that $p(w)$ is indeed the solution to the Fokker-Planck equation.

$$\begin{aligned}
 \lambda \frac{d}{dw} \left[\frac{dL}{dw} p(w) \right] + \frac{\lambda^2}{2S} \frac{d^2}{dw^2} [C(w)p(w)] &= \lambda \frac{d}{dw} \left\{ w \exp[-(w - w_0)^2] \right\} + \frac{\lambda^2}{2S} \frac{d^2}{dw^2} \left\{ c_0 - \frac{2S}{\lambda} \int \exp[-(w - w_0)^2] d\frac{1}{2}w^2 \right\} \\
 &= \lambda \frac{d}{dw} \left\{ w \exp[-(w - w_0)^2] \right\} - \lambda \frac{d}{dw} \left[w \exp[-(w - w_0)^2] \right] \\
 &= 0
 \end{aligned}$$

This example shows that, with proper noise, the stationary distribution and the landscape could even have different symmetry, and that it is possible to have a stationary distribution such that the expected gradient is non-vanishing.

The first example has been closely studied in the main text, and second example can be directly confirmed with a numerical simulation. See Figure 10.